

Gravitational Collapse of a Radiating Shell

G.L. Alberghi^{*,a}, R. Casadio^{†,a}, G.P. Vacca^{‡,a,b} and G. Venturi^{§,a}

^a *Dipartimento di Fisica, Università di Bologna and
Istituto Nazionale di Fisica Nucleare, Sezione di Bologna,
via Irnerio 46, 40126 Bologna, Italy*

^b *II Institut für Theoretische Physik, Universität Hamburg,
Luruper Chaussee 149, D-22761 Hamburg*

November 2, 2021

Abstract

We study the collapse of a self-gravitating and radiating shell of bosonic matter. The matter constituting the shell is quantized and the construction is viewed as a semiclassical model of possible black hole formation. It is shown that the shell internal degrees of freedom are excited by the quantum non-adiabaticity of the collapse and, consequently, on coupling them to a massless scalar field, the collapsing matter emits a burst of coherent (thermal) radiation. The backreaction on the trajectory is also estimated.

1 Introduction

Much effort has been dedicated to the study of the classical dynamics of gravitationally collapsing bodies and a fairly comprehensive understanding of the main features of this phenomenon is now available (see, *e.g.*, [1] and References therein). However, it is also clear that classical physics is not sufficient for a complete description, and for diverse reasons: first of all, the predicted point-like singularity which emerges as the final fate of the collapse is quantum mechanically unacceptable, just on the basis of naive consideration of the uncertainty principle; secondly, as soon as the collapsing body approaches its own gravitational radius, Hawking radiation [2] switches on and its backreaction should be included properly [3]. Moreover, the above two issues are connected, since Hawking's effect violates the positive energy condition which is a basic hypothesis of the singularity theorems [4]. One therefore expects corrections to the classical picture already at the semiclassical level, *i.e.*, in the region where matter is properly evolved by quantum equations on a space-time whose dynamics is still reliably approximated by classical equations.

^{*}e-mail: alberghi@bo.infn.it

[†]e-mail: casadio@bo.infn.it

[‡]e-mail: vacca@bo.infn.it

[§]e-mail: armitage@bo.infn.it

The semiclassical limit for various models has been previously investigated [5, 6, 7, 8, 9] by employing a Born-Oppenheimer (BO) decomposition of the corresponding minisuperspace wavefunction [10, 11, 12]. In particular, in Ref. [9] the case of a (thin) shell of quantized scalar matter collapsing in vacuum was investigated and it was shown that the collapse induces the production of matter quanta. Further, explicit conditions were found beyond which the semiclassical approximation breaks down. Such a model is, however, both unrealistically simple and of little physical use, since the absence of any signal from the shell precludes an observer from witnessing the process. In order to overcome the latter shortcoming, an effective minisuperspace action for radiating shells was derived in Ref. [13] as the first step in the modelling of a more realistic case. This was expected to be useful both for the conceptual problem of unambiguously quantizing the system and for obtaining more predictive conclusions: in fact, the possibility of adding an observer (*e.g.*, in the form of a detector coupled to the outgoing radiation) allows one to define physical (and not just formal) observables [14].

As mentioned above, one of the most intriguing aspects of collapsed bodies is the outgoing flux of thermal radiation predicted by Hawking [2]. This effect is usually studied in the background of a preexisting black hole, thus separating the problem of the collapse from the understanding of the onset of the thermal radiation. Such an approach is inspired by Hawking's original computation, where any backreaction on the chosen Schwarzschild background is neglected and the matter collapsed to form the black hole plays no role, and is further supported by the smallness of the (renormalized) energy-momentum tensor of the radiation in the vicinity of the horizon [15]. In this framework, one can think of a particle-antiparticle pair being generated outside the (event [16] or apparent [3]) horizon, with the positive energy particle escaping in the form of thermal radiation and the negative energy antiparticle falling inside the horizon decreasing the ADM mass (*i.e.*, proper mass plus gravitational energy) of the singularity. It is therefore the horizon, a purely geometrical concept, which appears as the key ingredient for this process, and much attention is devoted to studying event horizons as if possessing physical degrees of freedom of their own [17, 18] (see also Refs. [19, 20] for more recent developments). However, on recalling that the central singularity is a transmutation of the collapsed body, one is alternatively tempted to define the Hawking effect as a transfer of energy from the ADM mass of the collapsing matter to the radiation field.

The latter statement can be put on a firmer ground if one considers the collapse and the onset of the Hawking radiation in the same and only picture, which is also the scheme we are naturally led to use if we take the point of view of a (distant) static observer. For such an observer the collapse would never end (classically) and the final fate of the collapsing body necessarily overlaps with the onset of thermal emission. Hence, the static observer does not see an intermediate stage at which there is a true black hole, because the infalling flux of negative energy annihilates against the (still) collapsing matter, and it is clear that he would consider the Hawking radiation as energy lost by the collapsing body when it approaches its own gravitational radius. In this scenario, the applicability of the no-hair theorems becomes questionable, with geometry playing (at most) a subsidiary role, and one should be able to describe the whole process in terms of dynamical quantities, in much the same fashion as is the case for non-gravitational interactions [21], and possibly recover unitarity [22, 23]. This approach was explored long ago in Refs. [24], whose authors were led to deny the very formation of black holes (horizons), and has been revived recently from purely kinematical arguments in the framework of optical geometry [25]. To summarize the present situation, it still sounds fair to say, as in Ref. [3], that the issue of whether the horizon forms or not requires a better

understanding of the (quantum mechanics of the) gravitational collapse.

Instead of constructing a general formalism, in the present paper we shall continue our study of a specific (quantum mechanical) model of collapsing bosonic matter, to wit, the *self-gravitating* shell (for a purely classical treatment see, *e.g.*, Ref. [26]). Given its wide flexibility as a building block for more complex configurations, we believe that the conclusions we are able to draw are sufficiently general to be taken as hints for other situations. One may query our use of a scalar field, rather than fermionic matter, for the collapse. Clearly, in our case one will have, besides some simplifications, effects associated with the matter’s Bose-Einstein nature, for example the formation of a condensate. Nonetheless, even if apparently unrealistic, considerable effort has been dedicated to the effects of such matter (*e.g.*, in the context of boson stars [27]).

Returning to our previous study of a collapsing self gravitating shell, we consider a “macroshell” constructed from a large number of “microshells”, each of which corresponds to the *s*-wave collapse of a scalar particle of typical hadronic mass ($m_h \sim 1$ GeV). In Ref. [9], we discussed how such microshells were bound together to form the macroshell and found the confining potential to be linear and dependent on the shell radius. This implied that as the macroshell collapses, the confined microshells undergo non-adiabatic transitions from the ground to higher excited states. The attitude we adopted is that, because of their bosonic nature, the microshells formed a “condensate” and that, once enough microshells were excited (thus widening the macroshell) they would collectively decay to the ground state by creating additional particles (in analogy with hadronic string theory wherein a long string – excited hadron decays into short strings – lighter hadrons). Thus during the collapse the creation of additional microshells (particles) leads to a backreaction slowing the macroshell.

It is clear that in the above the Schwarzschild (ADM) mass of the shell does not change. We previously indicated that a more realistic approach would be to consider non-adiabatic effects leading to transitions from the ground to the higher (excited) states for some of the bound microshells and, subsequently, these states would decay and the microshells would return to the ground state by emitting radiation [13, 14]. At the end of such a process, the proper energy of the macroshell would be essentially unchanged (except for the small change in ground state energy due to the change in macroshell radius) and the net balance is then a transfer of the gravitational energy of the macroshell to the radiation field which decreases the ADM mass of the system and modifies the trajectory for the radius of the macroshell.

In our present approach we do not consider particle (microshell) creation, which would require much greater energy than the excitations of the microshells due to non-adiabatic effects (in Ref. [9] we also showed that microshell creation occurs for rather extreme cases, in which the size of the horizon is comparable to the Compton wavelength of the microshells), but study the latter excitations. In order to determine the latter excited levels we must describe the motion of one microshell in the mean gravitational field of the others and obtain an effective Schrödinger equation for the microshell. Such a study is attempted in the next Section. Subsequently one must determine the amplitude for the excitation of a microshell, as a consequence of the time variation of the binding potential due to the collapse of the shell (this is attempted in Section 3.1). The model is constructed bearing in mind a number of constraints: firstly, since our scalar particles have a Compton wavelength of $\sim 10^{-14}$ cm, one must have both that the radius of the shell and the thickness of the macroshell be much greater, otherwise fluctuations due to the quantum nature of matter will destroy our semiclassical description of the macroshell motion (see the consistency conditions for the semiclassical approximation in our previous paper, Ref. [9]). This essentially implies that the number of microshells of hadronic mass be at least

10^{40} so that, for example, the gravitational radius is sufficiently large. Another constraint which will allow us to simplify our results is to suppose that the collapse be non-relativistic (*i.e.*, “slow” all the way down to the horizon), which implies that only the first microshell excited states will be relevant.

In the remainder of Section 3 we address the emission of the radiation (scalar massless particles – we shall subsequently just call them photons) and the macroshell trajectory with backreaction. Again we shall enforce some constraints, in particular that the coupling of the radiation to the microshells be sufficiently large so that the decay time is smaller than the unperturbed collapse time. Actually, we shall see that such is already the case for a very small coupling constant. Further, interesting features of the model are that the collapse is slow and the shell tickness remains much smaller than the typical wavelength of the emitted quanta, so that many emissions occur practically in phase, thus rendering the radiation process highly coherent and the backreaction great. As a consequence, it will be sufficient for us to just consider first order perturbation theory in the radiation coupling constant and keep terms to lowest order in the macroshell velocity.

One may wonder if our model is useful in describing Hawking’s radiation, which has two main features: the first one is the thermal spectrum and the second one is its “observer dependence”. The former follows from the adiabatic hypothesis that the ADM mass of the source (black hole) changes slowly in time and, therefore, one does not necessarily expect to recover a thermal spectrum in a fully dynamical context in which the backreaction is included. By the latter we mean that a freely falling observer remains in its initial state all the time and should thus not experience the flux of outgoing energy measured by a static observer, regardless of the adiabatic approximation. We just point out that our model shows such a sort of “observer dependence”, since the proper mass, which remains constant, is the energy as measured by the observer comoving with the shell which, in turn, does not experience any change. At the same time there is a flux of outgoing radiation associated with the decrease of the ADM (Bondi) mass. However, whether such a radiation can be consistently identified with Hawking’s or should be considered as a totally different effect will need further inspection. Let us note in any case that, in contrast with Hawking radiation, the coupling constant of the radiation to the microshells will appear in the final expressions.

Naturally our results will also be constrained by our availability of computing power: bearing all the above points (and approximations) in mind, our results are illustrated and summarized in the Conclusions.

We use units for which $c = 1$ but explicitly show both Newton’s constant G and Planck’s constant \hbar . The Planck length and mass are then given by $\ell_p^2 = \hbar G$ and $m_p = \hbar/\ell_p$.

2 The macroshell inner structure

In order to study realistically the evolution of a collapsing body it is important not to neglect its spatial structure. For instance, the equivalence principle implies that a point-like freely falling observer does not experience any gravitational effect. However, any object has a spatial extension and tidal forces become effective when this size gets close to the typical scale of variation of the space-time curvature. At the same time, it is also important to keep the model simple so as to allow one to study it. A good compromise between realism and simplicity is given by the *macroshell* which was introduced in Ref. [9] and which we now review and further develop.

We view the collapsing shell not just as a singular spherical surface in space [28] but as a set of a large number N of *microshells* which correspond to collapsing s -wave bosons and are described by a wavefunction (thus the microshell radius is actually the “average” radius). Each microshell has negligible thickness and proper mass m such that their total proper mass equals the proper mass of the macroshell, $Nm = M$. If we denote by $r \in (0, +\infty)$ the usual “areal” radial coordinate, we can order the microshells according to their area, so that $r_1 < r_2 < \dots < r_N$, and assume that the thickness δ of the macroshell is small,

$$0 < \delta \equiv r_N - r_1 \ll r_1 . \quad (2.1)$$

The space between each two microshells has Schwarzschild geometry,

$$ds_i^2 = - \left(1 - \frac{2G M_i}{r} \right) dt_i^2 + \left(1 - \frac{2G M_i}{r} \right)^{-1} dr^2 + r^2 d\Omega^2 , \quad (2.2)$$

with a suitable ADM mass $M_i < M_{i+1}$, $M_0 = 0$ for $r < r_1$ and $M_N \equiv M_s$ (total ADM mass) for $r > r_N$. For this description to be consistent, one must check that the microshells do not spread during the collapse and δ remains small in the sense specified above. This was already shown in Ref. [9] to be ensured by the mutual gravitational interaction of the microshells if N is sufficiently large and the average radius of the shell R is much larger than the gravitational radius $R_H \equiv 2G M_s$. We shall provide further evidence for this in the following.

Before studying the dynamics of the microshells, one must also “fix the gauge” corresponding to the freedom of making coordinate transformations on the relevant solution (2.2) of the Einstein field equations. This can be done by choosing an ADM foliation [29] for the corresponding space-time manifold. Two options which cover the domain of outer communication (the region outside the horizon) are given by the hypersurfaces $\{\Sigma_\tau\}$ of constant proper time τ , associated with observers comoving with the microshells, and the hypersurfaces $\{\Sigma_t\}$ of constant Schwarzschild time (denoted by $t_\infty \equiv t_N$) which are associated with (distant) static observers¹. Since we shall consider only bound orbits for the shell with initially large radius and negligible velocity, it is useful, in this respect, to separate the collapse in the *Newtonian regime* (NR) and the *near horizon regime* (NHR):

NR) when the radius of the shell is large (and its velocity small), the difference between the proper time of the microshells and the Schwarzschild time is negligible, meaning that observers comoving with microshells at different radii can synchronize their clocks with the clock of the distant observer. Therefore, one expects that the Hilbert space which contains states of the microshells as viewed by the comoving observers, $\mathcal{H}_\tau = \{\Phi^{(\tau)}(r, \tau)\}$, is the same as $\mathcal{H}_t = \{\Phi^{(t)}(r, t_\infty)\}$ viewed by the (distant) static observer. We examine this case in Appendix A.

NHR) near the gravitational radius, the relative gravitational red-shift between different parts of the macroshell is no longer negligible and the two foliations $\{\Sigma_\tau\}$ and $\{\Sigma_t\}$ differ significantly, since $t_\infty = t_\infty(r, \tau)$ is a large transformation there [see Eq. (B.4)]. One can still introduce an Hilbert space \mathcal{H}_τ as relevant for the comoving observers, and a space \mathcal{H}_t for

¹Strictly speaking, the domain of outer communication is well defined only provided one knows the development of the whole space-time manifold [4]. However, in our case we cannot know from the beginning whether an event horizon will form or not and, thus, if $\{\Sigma_t\}$ can cover just a portion or the whole of space-time. At the same time, $\{\Sigma_\tau\}$ is defined naturally just on the world-strip where the macroshell has support.

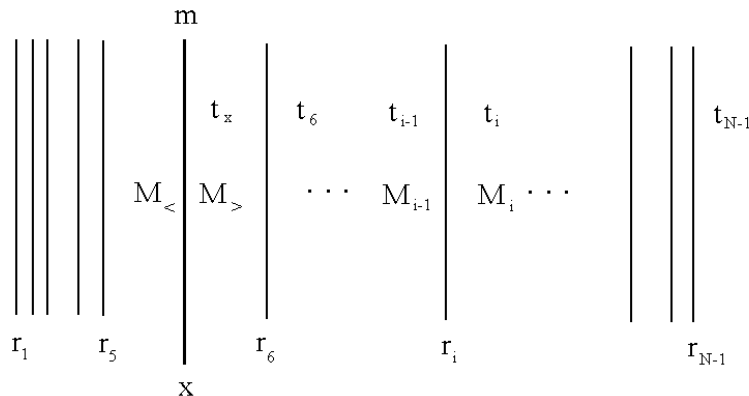


Figure 1: The macroshell structure.

the distant observer, but the relation between the two spaces (or their physical equivalence) is far from trivial, as will be apparent from the corresponding Schrödinger equations we display below and in Appendix B (see, *e.g.*, Refs. [30, 23] for analogous considerations).

In NR there is no conceptual ambiguity, since the Newtonian (Schwarzschild) time (equal to the proper time) is a Killing vector with respect to which canonical quantization is straightforward and most calculations can then be completed analytically (see, *e.g.*, Appendix A and Ref. [9]). Instead, in NHR there is no *a priori* reason to prefer either of the two Hilbert spaces to describe properly the matter in the shell. Further, if one were to neglect the backreaction on the metric and study a shell evolving on a fixed (Schwarzschild) background, the Schwarzschild time would still be a Killing vector and provide a unique way for canonical quantization. However, if one considers a collapsing macroshell with a microshell structure in order to successively include backreaction, the canonical analysis is much more involved and ambiguous.

In the spirit of locality, it seems natural (and also appears much easier) to analyse bound states of microshells with the aid of \mathcal{H}_τ and then move on to the point of view of the static observer by simply making a change of time coordinate (after having taken the thin shell limit). However, in so doing one does not expect to recover the space \mathcal{H}_t obtained prior to the thin shell limit, nor is it obvious whether the Principle of Equivalence, in any of its forms [31], can be trusted for length scales associated with such bound states which are of the order the Compton wavelength of (elementary) particles. In the present paper, we shall motivate taking the thin shell limit at some point by studying the trajectory of the shell only down to a radius greater than the gravitational radius (horizon) by several shell thicknesses.

In order to define an effective Hamiltonian for each microshell, let us single out one of the N microshells, denote its radius by x and study its motion in the background defined by the remaining $N - 1$ microshells (see Fig. 1). When $x \neq r_i$, one can apply the junction conditions [28] which yield

$$\left(\frac{dx}{d\tau_x}\right)^2 = -1 + \frac{(M_> - M_<)^2}{m^2} + G \frac{M_> + M_<}{x} + \frac{G^2 m^2}{4x^2} \equiv F(x), \quad (2.3)$$

where $M_<$ ($M_> \equiv M_x$) is the ADM mass computed on the inner (outer) surface of the microshell

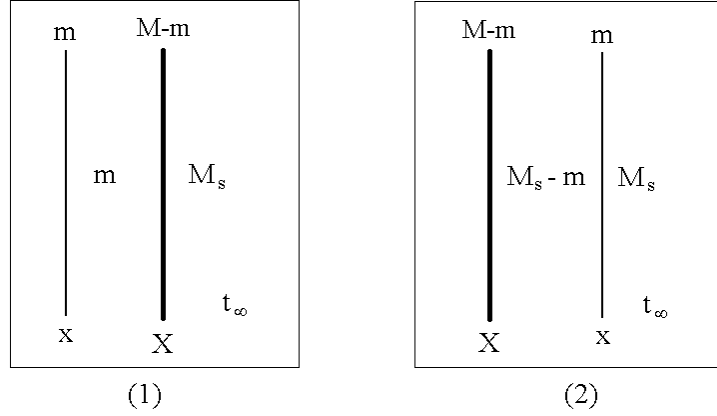


Figure 2: The equivalent configuration when the microshell lies outside the macroshell: (1) $x < X$; (2) $X < x$.

and τ_x is the proper time of the microshell. Then, on multiplying Eq. (2.3) by $m/2$ one will obtain the equation of motion for a microshell in the form of an effective Hamiltonian constraint

$$H_m \equiv \frac{1}{2} m \left(\frac{dx}{d\tau_x} \right)^2 + V = 0 . \quad (2.4)$$

Since $m \ll M$, we shall take $M_> - M_< \simeq m$, which amounts to $dx/d\tau_x \simeq 0$ for large x ($\gg R_H$) and is consistent with the choice of having the microshells confined within the thickness δ at large radius. With this assumption both $M_>$ and $M_<$ become functions of the microshells distribution $\{r_i, M_i\}$ only, but the evaluation of V remains extremely involved because one should first determine the most likely set of $2(N-1)$ values $\{r_i, M_i\}$.

One can get an approximate expression for V by making careful use of the thin shell limit ($\delta \ll r_1$) and considering the form of the potential when $x < r_1$ or $x > r_1 + \delta$. In this case, if we denote by X the (average) radius of the macroshell of proper mass $M - m$, we can also supplement Eq. (2.3) with the analogous expression for the macroshell. For $x < X$ [see case (1) in Fig. 2] one then has

$$\left(\frac{dx}{d\tau} \right)^2 = \frac{Gm}{x} + \frac{G^2 m^2}{4x^2} \equiv F_<(x) \quad (2.5)$$

$$\left(\frac{dX}{d\tau} \right)^2 = -1 + \left(\frac{M_s - m}{M - m} \right)^2 + G \frac{M_s + m}{X} + G^2 \frac{(M - m)^2}{4X^2} \equiv F_<(X) ,$$

where we have equated the proper times of the two shells in agreement with our choice of foliating the space-time into spatial slices Σ_τ parameterized by the local time of the microshells. Analogously, for $X < x$ [see case (2) in Fig. 2]

$$\left(\frac{dx}{d\tau} \right)^2 = G \frac{2M_s - m}{x} + \frac{G^2 m^2}{4x^2} \equiv F_>(x) \quad (2.6)$$

$$\left(\frac{dX}{d\tau}\right)^2 = -1 + \left(\frac{M_s - m}{M - m}\right)^2 + G \frac{M_s - m}{X} + G^2 \frac{(M - m)^2}{4 X^2} \equiv F_>(X) .$$

One is now ready to define the relative and centre-mass radius according to

$$\begin{aligned} \bar{r} &\equiv x - X \\ R &\equiv \frac{m}{M} x + \frac{\mu}{M} X , \end{aligned} \tag{2.7}$$

where $\mu \equiv m(M - m)/M$ is the reduced mass of the system. The above relations can then be inverted and, upon substituting into Eqs. (2.5) and (2.6), one obtains an effective Hamiltonian for the two shells given by

$$H^{(\tau)} = \frac{1}{2} M \left(\frac{dR}{d\tau}\right)^2 + \frac{1}{2} \mu \left(\frac{d\bar{r}}{d\tau}\right)^2 + V^{(\tau)} \equiv H_M^{(\tau)} + H_m^{(\tau)} . \tag{2.8}$$

The potential contains the following relevant terms

$$V_m^{(\tau)} = \frac{G M_s m}{2 R} \frac{\bar{r}}{R} \times \begin{cases} \left(1 - \frac{G M^2}{2 R M_s}\right) & \bar{r} > +\frac{\delta}{2} \\ \left(-1 - \frac{G M^2}{2 R M_s}\right) & \bar{r} < -\frac{\delta}{2} , \end{cases} \tag{2.9}$$

where we have also assumed $m \ll M_s (\leq M)$ and neglected all non-leading terms in m . The assumption $M_s \gg m$, although is not guaranteed *a priori*, has been done here just for the purpose of simplifying the displayed expressions. However, we shall show in Section 3.4 that it actually holds true all along the collapse in all the cases of interest.

At this point, one can use the external potential to shape the distribution of microshells inside the macroshell and construct the potential $V^{(\tau)}$ for $|\bar{r}| < \delta/2$ (see Appendix A for an explicit calculation in NR). By expanding the latter potential in powers of δ/R and neglecting terms of order $(\delta/R)^2$ or higher, one finally obtains an effective Hamiltonian for each microshell,

$$H_m^{(\tau)} = \frac{1}{2} m \left(\frac{d\bar{r}}{d\tau}\right)^2 + V_m^{(\tau)} , \tag{2.10}$$

with a potential function which interpolates smoothly ² between the two linear in \bar{r} (outer) parts of the potential given by $V_m^{(\tau)}$ in Eq. (2.9),

$$V_m^{(\tau)} = \frac{G M_s m}{2 R^2} \left(\frac{\bar{r}^2}{\delta} + \frac{\delta}{4}\right) - \frac{G^2 M^2 m}{4 R^3} \bar{r} , \quad |\bar{r}| \leq \frac{\delta}{2} . \tag{2.11}$$

We then observe that for $R \gg R_H \sim 2 G M$ the term linear in \bar{r} is negligible and the potential is thus symmetric around the average radius of the macroshell, but for $M_s < M$ it becomes steeper for $\bar{r} < 0$ and flattens out for $\bar{r} > 0$ (see Fig. 3 for the case of $N = 10^{40}$ protons and δ of the order of the Compton wavelength ℓ_h of the proton). The same effect happens for decreasing values of the average radius at fixed ratio M/M_s (see Figs. 4 and 5; note that, for this choice of M , the potential confines all the way down to R_H).

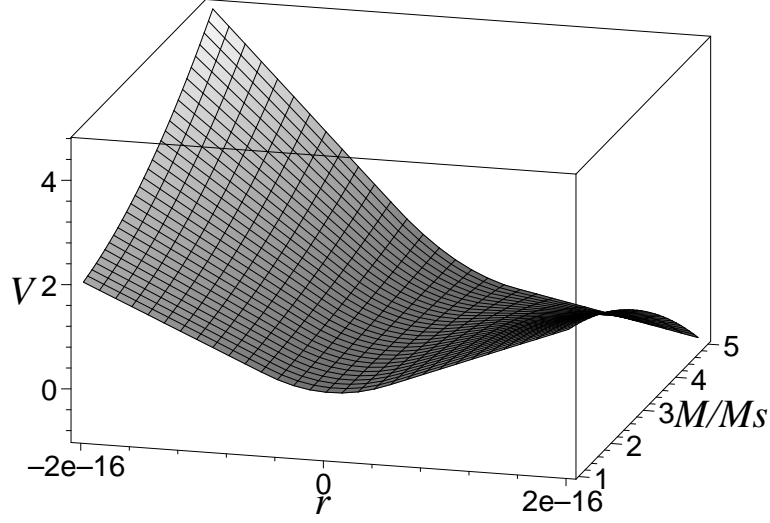


Figure 3: The potential $V^{(\tau)}$ for $M = 10^{40} m_h$, $R = 4 R_H = 10^{-13} \text{ m}$, $\delta \sim \ell_h = 10^{-16} \text{ m}$, $-\delta < \bar{r} < \delta$ and $1 \leq M/M_s \leq 5$. Vertical units are arbitrary.

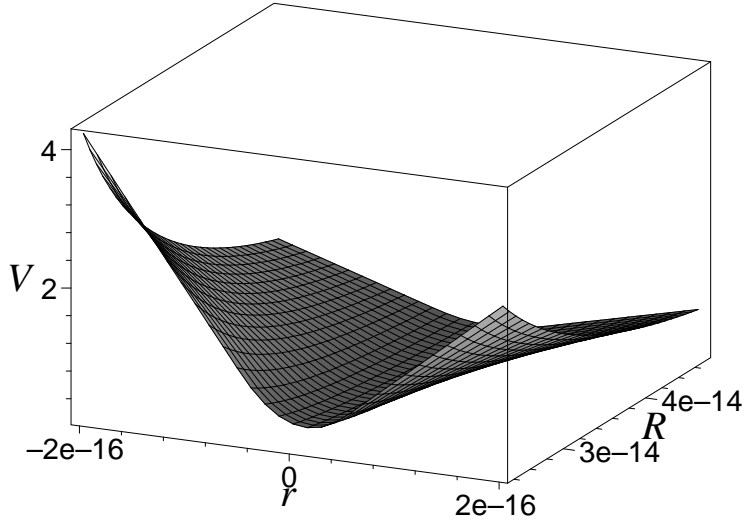


Figure 4: The potential $V^{(\tau)}$ for $M = M_s = 10^{40} m_h$, $\delta \sim \ell_h = 10^{-16} \text{ m}$, $-\delta < \bar{r} < \delta$ and $R_H < R < 2 R_H$. Vertical units are arbitrary.

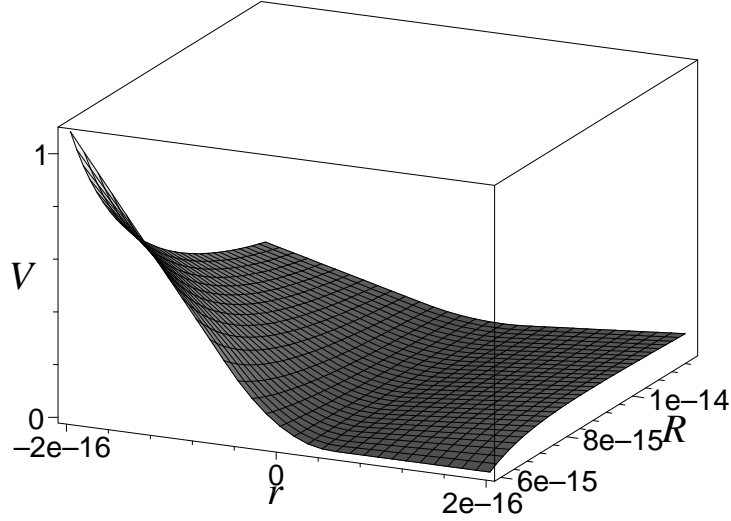


Figure 5: The potential $V^{(\tau)}$ for $M = M_s = 10^{40} m_h$, $\delta \sim \ell_h = 10^{-16} \text{ m}$, $-\delta < \bar{r} < \delta$ and $R_H/4 < R < R_H/2$. Vertical units are arbitrary.

For a comparison with the case when the space-time is foliated into slices Σ_t parameterized by the Schwarzschild time t_∞ measured by a (distant) static observer we refer to Appendix B. There we show how to obtain the relevant potential $V_m^{(t)}$ as an expansion in powers of G . Then, since $V_m^{(t)}$ contains terms of all orders in G , while $V_m^{(\tau)}$ goes only up to $\mathcal{O}(G^2)$, this comparison clearly confirms that perturbative methods cannot always be trusted when dealing with strong gravitational fields or, if we wish, the disadvantage of using the Schwarzschild rather than proper time. In the same Appendix we show that, if one takes the thin shell limit of $V_m^{(\tau)}$ and then changes to the Schwarzschild time multiplying by $(d\tau/dt_\infty)^2$, one recovers the thin shell limit of $V_m^{(t)}$ in NR. This means the two steps of introducing a potential and taking the thin shell limit commute (as expected) in NR.

For $R \gg R_H$ and $M \sim M_s$, the potential V_m is symmetric around $\bar{r} = 0$. This confines the microshells within the following thickness [9] (see also Appendix C for more details on the spectrum of bound states)

$$\delta \sim \frac{\ell_m}{(2N)^{1/3}} \left(\frac{R}{\ell_p} \right)^{2/3} \sim \ell_m^{2/3} R^{1/3} \left(\frac{R}{R_H} \right)^{1/3}, \quad (2.12)$$

where $\ell_m = \hbar/m$ is the Compton wavelength of a microshell. For R close to R_H or smaller ratios of M_s/M the potential twists (see Figs. 5 and 3) and, eventually, ceases to confine the microshells on the outside if the macroshell shrinks below the gravitational radius [see Eq. (C.14)]. We further note that the spreads of the lowest wavefunctions are also of order δ , thus the bosonic

²We assume there is no discontinuity experienced by the test microshell when it crosses the borders of the macroshell and equate the first derivative of the quadratic potential to the first derivative of the linear potential at $|\bar{r}| = \delta/2$.

microshells are essentially superimposed and form a condensate, hence some classical singular behaviour, such as microshell crossings, do not occur.

Let us now summarize what we have done in simple quantum mechanical terms. Since we are considering wavefunctions, we have viewed each microshell as immersed in a continuous matter distribution, corresponding to the mean field of the others which are then treated as a (wide) single shell (Hartree approximation or independent particle model - see also the Thomas-Fermi model of the atom [32, 9]). Then we noted that, inside the macroshell, a microshell can undergo small displacements (δ/R is small) about equilibrium, which will be harmonic, and on requiring continuity with the potential outside the shell one obtains Eq. (2.11). Further, since in the context of our Hartree approximation the total wavefunction is just the product of the individual ones ³, it will be sufficient in what follows to just exhibit the Lagrangian and Hamiltonian for a given microshell.

3 The radiation and backreaction

In this Section we use the description of the macroshell as given in Section 2 and add the coupling to an external radiation field. This will allow the shell to radiate away any excess of the proper energy induced by the non-adiabaticity of the collapse, as outlined in the Introduction.

Our aim is to evaluate the flux of emitted radiation, which will determine $M_s = M_s(\tau)$, and the corresponding backreaction on the trajectory $R = R(\tau)$. We shall first estimate the non-adiabatic amplitude of excitation and, subsequently, give a purely quantum mechanical (coherent) treatment of the entire process of excitation and emission by coupling explicitly the microshell modes Φ_n to the radiation field. The outcome will be a set of two coupled ordinary differential equations (for R and M_s) which we shall solve numerically.

3.1 The excitation amplitude

From the previous Section we know that the microshells are governed by the Schrödinger equation (see also Appendix C)

$$i \hbar \frac{\partial \Phi_s}{\partial \tau} = \hat{H}_m^{(\tau)} \Phi_s \quad (3.1)$$

with

$$\hat{H}_m^{(\tau)} = \frac{\hat{\pi}_r^2}{2m} + V_m^{(\tau)} , \quad (3.2)$$

where $V_m^{(\tau)}$ is given in Eq. (2.11) and has an explicit time dependence due to $R = R(\tau)$. This type of equation can be solved by making use of invariant operators $\hat{I} = \hat{I}(\tau)$ which satisfy [33]

$$i \hbar \frac{\partial \hat{I}}{\partial \tau} + [\hat{I}, \hat{H}_m^{(\tau)}] = 0 . \quad (3.3)$$

The general solution $\Phi_s = \Phi_s(\tau)$ can then be written in the form

$$| \Phi, \tau \rangle_{Is} = \sum_n c_n e^{i \varphi_n} | n, \tau \rangle_I , \quad (3.4)$$

³Let us also remember that the many-boson wavefunction is symmetric.

where $|n, \tau\rangle_I$ is an eigenvector of \hat{I} with time-independent eigenvalue λ_n and the c_n are complex coefficients. We also recall that the phase $\varphi_n = \varphi_n(\tau)$ is given by the sum of the geometrical and dynamical phases,

$$\varphi_n = \frac{i}{\hbar} \int_{\tau_0}^{\tau} \langle n, \tau' | \hbar \partial_{\tau'} + i \hat{H}_m^{(\tau)} | n, \tau' \rangle_I d\tau' . \quad (3.5)$$

The Hamiltonian in Eq. (3.1) describes a harmonic oscillator of fixed mass m and variable frequency

$$\Omega = \frac{1}{R} \sqrt{\frac{R_H}{2\delta}} . \quad (3.6)$$

Hence, one can introduce standard annihilation and creation operators \hat{a} and \hat{a}^\dagger ,

$$\hat{a} = \sqrt{\frac{m\Omega}{2\hbar}} \left(\bar{r} + \frac{i\hat{\pi}_r}{m\Omega} \right) , \quad (3.7)$$

with $[\hat{a}, \hat{a}^\dagger] = 1$ and define the vacuum state as

$$\hat{a} |0, \tau\rangle_a = 0 \quad (3.8)$$

A complete set of eigenstates $\mathcal{A} = \{|n, \tau\rangle_a\}$ is then given by

$$|n, \tau\rangle_a = \frac{(\hat{a}^\dagger)^n}{\sqrt{n!}} |0, \tau\rangle_a , \quad (3.9)$$

where

$$\hat{a} |n, \tau\rangle_a = \sqrt{n} |n-1, \tau\rangle_a \quad (3.10)$$

$$\hat{a}^\dagger |n, \tau\rangle_a = \sqrt{n+1} |n+1, \tau\rangle_a .$$

The solutions of the corresponding time-independent problem obtained by assuming R constant and displayed in Appendix C are here recovered as $\Phi_n^{(2)}(\bar{r}) = \langle \bar{r} | n, 0 \rangle_a$.

One can also introduce the linear (non-Hermitian) annihilation and creation invariants \hat{b} and \hat{b}^\dagger [33, 34],

$$\hat{b} = \frac{1}{\sqrt{2\hbar}} \left[\frac{\bar{r}}{x} + i(x\hat{\pi}_r - m\dot{x}\bar{r}) \right] , \quad (3.11)$$

where $[\hat{b}, \hat{b}^\dagger] = 1$ and the function $x = x(\tau)$ is a solution of ⁴

$$\ddot{x} + \Omega^2 x = \frac{1}{m^2 x^3} , \quad (3.12)$$

with suitable initial conditions. The system then admits an invariant ground state defined by

$$\hat{b} |0, \tau\rangle_b = 0 , \quad (3.13)$$

⁴A dot denotes derivative with respect to τ throughout the paper.

from which one can build a basis of invariant eigenstates $\mathcal{B} = \{|n, \tau\rangle_b\}$,

$$|n, \tau\rangle_{bs} \equiv e^{i\varphi_n} \frac{(\hat{b}^\dagger)^n}{\sqrt{n!}} |0, \tau\rangle_b = e^{i\varphi_n} |n, \tau\rangle_b, \quad (3.14)$$

where

$$\begin{aligned} \hat{b} |n, \tau\rangle_b &= \sqrt{n} |n-1, \tau\rangle_b \\ \hat{b}^\dagger |n, \tau\rangle_b &= \sqrt{n+1} |n+1, \tau\rangle_b. \end{aligned} \quad (3.15)$$

We can then introduce the invariant number operator (in analogy with the standard number operator $\hat{a}^\dagger \hat{a}$)

$$\hat{I}_c = \hat{b}^\dagger \hat{b}. \quad (3.16)$$

The two basis \mathcal{A} and \mathcal{B} are related by Bogoliubov coefficients according to

$$\begin{cases} \hat{a} = B^* \hat{b} + A^* \hat{b}^\dagger \\ \hat{a}^\dagger = B \hat{b}^\dagger + A \hat{b} \end{cases} \Leftrightarrow \begin{cases} \hat{b} = B \hat{a} - A^* \hat{a}^\dagger \\ \hat{b}^\dagger = B^* \hat{a}^\dagger - A \hat{a} \end{cases}, \quad (3.17)$$

where

$$\begin{aligned} A &= \frac{1}{2} \sqrt{m\Omega} \left[\left(x - \frac{1}{m\Omega x} \right) - i \frac{\dot{x}}{\Omega} \right] \\ B &= \frac{1}{2} \sqrt{m\Omega} \left[\left(x + \frac{1}{m\Omega x} \right) - i \frac{\dot{x}}{\Omega} \right]. \end{aligned} \quad (3.18)$$

Further, \mathcal{A} and \mathcal{B} will coincide at $\tau = 0$ if

$$\hat{b}(0) = \hat{a}(0) \Rightarrow \hbar \Omega \left(\hat{I}_c(0) + \frac{1}{2} \right) = \hat{H}_m(0), \quad (3.19)$$

that is $A(0) = 0$ and $B(0) = 1$, which means that for the function x we must require

$$\begin{cases} x(0) = \frac{1}{\sqrt{m\Omega(0)}} \\ \dot{x}(0) = 0. \end{cases} \quad (3.20)$$

Since $\dot{\Omega} \sim \dot{R}$ and $\dot{R}(0) \simeq 0$, an approximate solution to Eq. (3.12) compatible with the initial conditions in Eq. (3.20) is given by

$$x \simeq \frac{1}{\sqrt{m\Omega}} \Rightarrow \dot{x} \simeq -\frac{\dot{\Omega}}{2\sqrt{m\Omega^3}}, \quad (3.21)$$

provided τ is sufficiently short so that \ddot{x} is negligible. The corresponding Bogoliubov coefficients are then given by

$$A \simeq -\frac{i\dot{\Omega}}{4\Omega^2}, \quad B \simeq 1 + A, \quad (3.22)$$

and satisfy the unitarity condition

$$|B|^2 - |A|^2 = 1 . \quad (3.23)$$

The amplitude of the transition from the state Φ_0 to Φ_n after the time $\tau \geq 0$ can be easily computed. In particular, one finds [33]

$$\begin{aligned} A_{0 \rightarrow 2n}(\tau) &= {}_a \langle 2n, \tau | 0, \tau \rangle_b \\ &= \frac{1}{\sqrt{B}} \left(\frac{A^*}{B} \right)^n \frac{\sqrt{(2n)!}}{2^n n!} \end{aligned} \quad (3.24)$$

$$\begin{aligned} A_{0 \rightarrow 2n+1}(\tau) &= {}_a \langle 2n+1, \tau | 0, \tau \rangle_b \\ &= 0 . \end{aligned} \quad (3.25)$$

To leading order in $|A|$ (*i.e.*, $\dot{\Omega} \sim \dot{R}$), one then has $A_{0 \rightarrow 0}(\tau) \simeq 1$ and the amplitude of the transition to the excited state with energy $E_{2n} = E_0 + 2n \hbar \Omega$ is

$$\begin{aligned} A_{0 \rightarrow 2n}(\tau) &\simeq i^n \frac{\sqrt{(2n)!}}{2^{3n} n!} \frac{\dot{\Omega}^n(\tau)}{\Omega^{2n}(\tau)} \\ &= (-i)^n \frac{\sqrt{(2n)!}}{3^n 2^{n/2} n!} \left(\frac{\delta}{R_H} \right)^{n/2} \dot{R}^n(\tau) , \end{aligned} \quad (3.26)$$

where we have assumed $R_H = 2GM_s$ remains constant in the interval $(0, \tau)$. The relevant expression for us is thus given by Eq. (3.26), in which we recall that $\dot{R} < 0$. We also remark that the above transition amplitude follows as both a non-adiabatic effect (since $A_{0 \rightarrow 2n} \propto \dot{R}^n$) and a consequence of the finite thickness of the macroshell (since $A_{0 \rightarrow 2n} \propto \delta^{n/2}$), the latter being further related to the quantum mechanical nature of the bound states [since $\delta \propto \hbar^{2/3}$].

An order of magnitude estimate for the most probable transition ($2n = 2$) can be obtained by setting $\dot{R}^2 \sim GM_s/R$ and using Eq. (2.12), in which case

$$|A_{0 \rightarrow 2}(R, N)|^2 \leq |A_{0 \rightarrow 2}(R_H)|^2 \sim \left(\frac{\ell_m}{\ell_p} \right)^{4/3} \frac{1}{N^{2/3}} , \quad (3.27)$$

where we also approximated M_s as Nm in order to obtain a function of just the number N of microshells. Further, one can also check that the above probability is less than one and, for realistic cases, quite small (we shall exhibit this later). This implies that the probability for a microshell to get excited a second time (after it has radiated away the energy E_2 once, see next Section) is negligible and, considering also that the emission probability is small, we shall not consider double emission. We further note that, as expected, the larger R_H the smaller the “tidal” effects and the excitation amplitude.

3.2 The (thermal) radiation

The problem of coupling a radiation field in the form of a conformal scalar field to collapsing matter was previously treated in Ref. [5] (see also Ref. [6]) for the case of a collapsing sphere of dust, for which we recovered the Hawking temperature in a suitable approximation. For the present situation, we shall find it more convenient to use the analogy with an accelerated observer in flat space-time as put forward in Ref. [35].

The basic observation is that, if the proper mass or the ADM mass (or both) vary with time, the collapse of the shell is not a free fall. This can be seen very easily by noting that the solutions to the equation of motion (2.3) when $M_>$ and/or m depend on time differ from the case when the same parameters are constant. Alternatively, one can use the second junction condition [28] to compute the surface tension \mathcal{P} of the shell. As we have shown in the previous Section, the proper mass M of the shell increases in time, therefore, although our choice of initial conditions for R , M and M_s are such that $\mathcal{P}(0) = 0$, the tension subsequently increases when M increases. The tension then slows down the collapse [9], and this effect should be further sustained by the emission [13], which very quickly brings the proper mass back to the initial value. As we outlined in the Introduction, we shall then consider M as effectively constant along the collapse and compute the net variation of M_s in time.

Let us denote by

$$a = \ddot{R} - \ddot{R}_{\text{free}} , \quad (3.28)$$

the difference between the actual acceleration \ddot{R} of the shell and that of a freely falling body, \ddot{R}_{free} , having the same radial position R and proper velocity \dot{R} . Of course, a would equal the surface gravity,

$$a_H = \frac{1}{4GM_s} , \quad (3.29)$$

of a black hole of mass M_s for $R = R_H$ constant. In this limiting case, one could exploit the analogy between Rindler coordinates for an accelerated observer in flat space-time and Schwarzschild coordinates for static observers in a black hole background [15] and find that the shell emits the excess energy with the Hawking temperature

$$T_H = \frac{\hbar a_H}{2\pi k_B} , \quad (3.30)$$

where k_B is the Boltzmann constant (an explicit construction which leads to this result was proposed in Ref. [5]). In general, however, the effective acceleration a will have no *a priori* fixed relation with M_s and one should keep it as an independent function of τ to be determined later consistently with the equation of motion of the shell. It is also clear that, should \dot{R} turn out to be constant, a will correspond to the acceleration associated with the instantaneous ADM mass and distance from the horizon.

We then consider an isotropic massless scalar field φ conformally coupled to gravity [15] and to the microshells. The Lagrangian density for a given microshell and the radiation field is given by

$$\begin{aligned} \mathcal{L} = & +\frac{1}{r^2} \sum_{n \geq 0} \left[\frac{i\hbar}{2} \left(\Phi_n^* \dot{\Phi}_n - \dot{\Phi}_n^* \Phi_n \right) - \frac{\hbar^2}{2m} \frac{\partial \Phi_n^*}{\partial r} \frac{\partial \Phi_n}{\partial r} - V_m^{(\tau)} \Phi_n^* \Phi_n - e \sum_{l \neq n} \Phi_n^* \Phi_l \varphi \right] \\ & - \left[\partial_\mu \varphi \partial^\mu \varphi + \frac{1}{6} \mathcal{R} \varphi^2 \right] , \end{aligned} \quad (3.31)$$

where \mathcal{R} is the curvature scalar and $V_m^{(\tau)}$ is the potential given by Eqs. (2.9) and (2.11). The last term in the first square bracket represents minus the interacting Hamiltonian H_{int} with e the coupling constant of the radiation to a microshell while the wavefunctions of the latter are

expressed in terms of the states found in Appendix C as Φ_n/r , where we exhibit the energy levels ($n \geq 0$) so that the form of the interaction can be chosen in such a way that – to lowest order – it just contributes to the transition between different levels and does not modify the macroshell ground state energy. Further, the factor of $(1/r)$ comes from the normalization measure now being $r^2 dr$. In fact, in the thin shell limit it is consistent to approximate the metric on the shell with the outer Vaidya line element [36, 37]. Let us again note that we have just exhibited the Lagrangian for a given microshell since in the Hartree approximation the total wavefunction is just the product of the individual ones⁵.

Another important observation comes into play at this point. In the preceding Section we have computed the (non-vanishing) transition amplitudes $A_{0 \rightarrow 2n}$ to lowest order in \dot{R} , that is $\mathcal{O}(\dot{R})$ [see Eq. (3.26)], with M and M_s held constant. Therefore, in order to determine the flux of radiation to lowest order in \dot{R} , it is sufficient to compute the probability of emission to $\mathcal{O}(\dot{R}^0)$ with M and M_s constant. In this approximation (M_s constant), the Vaidya metric reduces to the Schwarzschild metric, so that the relevant four-dimensional measure of integration is

$$\sqrt{-g} d^4x \simeq r^2 \sin^2 \theta d\theta d\phi dr dt, \quad (3.32)$$

where t is the Schwarzschild time measured by a static observer (denoted by t_∞ in previous Sections),

$$t \sim \frac{\tau}{\sqrt{1 - R_H/R}}. \quad (3.33)$$

Finally, since the functions Φ_n are spherically symmetric and peaked near $r = R(\tau)$, it is convenient to integrate over the angular coordinates and write

$$\sqrt{-g} d^4x = 4\pi (R + \bar{r})^2 d\bar{r} dt, \quad (3.34)$$

where \bar{r} is the relative radial coordinate and $R = R(t)$ is the trajectory of the macroshell as before.

After the lapse of proper time τ , each microshell will jump into the excited state of energy $E_{2n} = E_0 + 2n\hbar\Omega$ with a transition amplitude $A_{0 \rightarrow 2n}(\tau)$. Successively, it can decay back to the ground state by emitting a quantum of energy $\hbar\omega$ (having a wavelength much larger than the shell thickness, see Table 1) of the scalar field. We shall later see that the macroshell velocity is small and the emissions are numerous. As a consequence, the distance covered between each emission is small with respect to the wavelength and therefore the emitted radiation will be coherent.

Let us now estimate, using first order perturbation theory in e , the transition amplitude for the emission of quanta of the scalar field, which will occur when the microshells in the state Φ_{2n} decay back to the ground state Φ_0 , for the interval between the times $t_1 \equiv t(\tau_1)$ and $t_2 \equiv t(\tau_2)$ ($0 < \tau_1 < \tau_2$). It will be given by

$$\begin{aligned} -\frac{i}{\hbar} \int_{t_1}^{t_2} dt \langle \text{final} | \hat{H}_{\text{int}} | \text{initial} \rangle &= -\frac{ie}{\hbar} \sum_{i=1}^N \int_{t_1}^{t_2} dt \langle 1_\omega; t | \hat{\varphi} | 0; t_1 \rangle \prod_{j=1}^N \langle j; 0; t | \\ &\quad \times \sum_{n \geq 0} \sum_{l \neq n} \hat{\Phi}_{i,n}^* \hat{\Phi}_{i,l} \sum_{s \geq 0} \prod_{r=1}^N |r, s; t\rangle \langle r, s; t | r, 0; 0 \rangle \end{aligned}$$

⁵Of course, both the total and the single particle wavefunctions are normalized to unity.

$$\simeq -\frac{4\pi i e}{\hbar} \sum_{i=1}^N \int_{t_1}^{t_2} dt \int d\bar{r}_i \Phi_0(\bar{r}_i) \Phi_2(\bar{r}_i) A_{i,0 \rightarrow 2}(t, 0) \\ \times e^{-2i\Omega\tau} \langle 1_\omega | \hat{\varphi}(R + \bar{r}_i, t) | 0 \rangle, \quad (3.35)$$

where $\langle i, n; t | i, 0; 0 \rangle = A_{i,0 \rightarrow n}(t)$ is the excitation amplitude (for the i^{th} microshell) which, as computed in the previous Section, is dominated by the contribution with $n = 2$ and for the photon state $|0\rangle$ we consider the Unruh vacuum, corresponding to an outgoing flux of radiation [15]. This of course implies that a is non-zero, indeed we shall actually find that $a \sim -\dot{R}_{\text{free}}$ (since $\ddot{R} \simeq 0$), consistently with our choice of vacuum and, near the horizon, the flux corresponds to Hawking radiation (see Ref. [38] for a detailed discussion of the analogy between Schwarzschild and Rindler spaces). Let us further note that, although a black hole is only close to being formed, it is generally accepted that it is the Unruh vacuum that best approximates the state that would be formed following the collapse of a massive body [15].

On taking the modulus squared of Eq. (3.35), one obtains the transition probability

$$P(2\Omega; t_2, t_1) \simeq \frac{16\pi^2 e^2}{\hbar^2} \sum_{i=1}^N \sum_{j=1}^N \int_{t_1}^{t_2} dt'' \int_{t_1}^{t_2} dt' \int d\bar{r}_i'' \int d\bar{r}_j' A_{i,0 \rightarrow 2}'' A_{j,0 \rightarrow 2}' e^{-i2(\Omega''\tau'' - \Omega'\tau')} \\ \times \Phi_0(\bar{r}_i'') \Phi_2(\bar{r}_i'') \Phi_2(\bar{r}_j') \Phi_0(\bar{r}_j') \langle 0 | \hat{\varphi}(R'' + \bar{r}_i'', t'') \hat{\varphi}(R' + \bar{r}_j', t') | 0 \rangle, \quad (3.36)$$

where $X' \equiv X(t')$, $X'' \equiv X(t'')$ for any function of time and the last term is the Wightman function for the scalar field φ .

The four-dimensional Wightman function can be related to its two-dimensional counterpart D_u^+ [15] through

$$\langle 0 | \hat{\varphi}(R'' + \bar{r}_i'', t'') \hat{\varphi}(R' + \bar{r}_j', t') | 0 \rangle = \frac{D_u^+(R'' + \bar{r}_i'', t''; R' + \bar{r}_j', t')}{4\pi(R'' + \bar{r}_i'')(R' + \bar{r}_j')} \\ = -\frac{\hbar}{16\pi^2} \frac{\ln[(\Delta v_{ij} - i\epsilon)(\Delta \bar{u}_{ij} - i\epsilon)]}{(R'' + \bar{r}_i'')(R' + \bar{r}_j')}, \quad (3.37)$$

where, of course, we only consider s -waves and

$$\Delta v_{ij} = t'' - t' + (R'' + \bar{r}_i'')_* - (R' + \bar{r}_j')_* \\ \simeq \Delta t + \frac{\bar{R}(\Delta R + \Delta \bar{r}_{ij})}{\bar{R} - R_H}. \quad (3.38)$$

In the above $r_* = r + R_H \ln[(r/R_H) - 1]$ is the turtle coordinate [29]. We also set $\Delta t = t'' - t'$ (similarly for ΔR and $\Delta \bar{r}$), $\bar{R} = (R'' + R')/2$ and assumed $\bar{R} - R_H \gg |\Delta R|, |\Delta \bar{r}_{ij}| = |\bar{r}_i - \bar{r}_j|$. Further,

$$\Delta \bar{u}_{ij} = -2R_H \left\{ \exp\left[-\frac{t'' - (R'' + \bar{r}_i'')_*}{2R_H}\right] - \exp\left[-\frac{t' - (R' + \bar{r}_j')_*}{2R_H}\right] \right\} \\ \simeq 2R_H \exp\left(\frac{\bar{R}_* - T - t_1}{2R_H}\right) \left\{ \exp\left[\frac{1}{2R_H} \left(\frac{\Delta t}{2} - \frac{\bar{R}(\bar{r}_i' + \Delta R/2)}{\bar{R} - R_H}\right)\right] \right. \\ \left. - \exp\left[\frac{1}{2R_H} \left(\frac{\bar{R}(\bar{r}_j'' + \Delta R/2)}{\bar{R} - R_H} - \frac{\Delta t}{2}\right)\right] \right\}, \quad (3.39)$$

where $T = (t' + t'')/2 - t_1$ and we have performed the same approximation as we used in obtaining Eq. (3.38).

The above expressions can be simplified on noting that one expects $\Delta t \gg \delta$, $\Delta R (= \dot{R} \Delta t \sqrt{1 - R_H/\bar{R}})$ corresponding to the fact that the wavelength of the emitted scalar quantum is much greater than the width of the shell and the velocity of the shell sufficiently small so that it is not displaced much between one emission and the next (see Table 1). One then obtains for Eqs. (3.38) and (3.39) respectively

$$\Delta v \simeq \Delta t \quad (3.40)$$

$$\begin{aligned} \Delta \bar{u} &\simeq 2 R_H \exp\left(\frac{\bar{R}_* - T - t_1}{2 R_H}\right) \left[\exp\left(\frac{\Delta t}{4 R_H}\right) - \exp\left(-\frac{\Delta t}{4 R_H}\right) \right] \\ &= 4 R_H \exp\left(\frac{\bar{R}_* - T - t_1}{2 R_H}\right) \sinh\left(\frac{\Delta t}{4 R_H}\right). \end{aligned} \quad (3.41)$$

On introducing $L = t_2 - t_1$, expressing Eq. (3.36) in terms of T and Δt and approximating the integration measure as in Eqs. (3.40) and (3.41) with

$$\begin{aligned} R' &= R(T) - \dot{R}(T) \sqrt{1 - R_H/\bar{R}} (\Delta t/2) \\ R'' &= R(T) + \dot{R}(T) \sqrt{1 - R_H/\bar{R}} (\Delta t/2), \end{aligned} \quad (3.42)$$

and $R(T) = \bar{R}$, one obtains to leading order in \dot{R}

$$\begin{aligned} P(2\Omega; t_1, L) &\simeq N^2 \frac{e^2 \hbar}{2 m^2} \int_0^L dT \frac{|A_{0 \rightarrow 2}|^2}{R^6 \Omega^2} \int_{-\Lambda}^{+\Lambda} d(\Delta t) e^{-i 2 \Omega \sqrt{1 - R_H/\bar{R}} \Delta t} \\ &\quad \times \ln \left[4 R_H e^{(R_* - T - t_1)/2 R_H} (\Delta t - i \epsilon) \sinh\left(\frac{\Delta t}{4 R_H} - i \epsilon\right) \right] \\ &\simeq N^2 \frac{e^2 \hbar}{2 m^2} \int_0^L dT \frac{|A_{0 \rightarrow 2}|^2}{R^6 \Omega^2} \int_{-\Lambda}^{+\Lambda} d(\Delta t) e^{-i 2 \Omega \sqrt{1 - R_H/\bar{R}} \Delta t} \\ &\quad \times \frac{(-i)}{2 \Omega \sqrt{1 - R_H/\bar{R}}} \left[\frac{1}{\Delta t - i \epsilon} + \frac{1}{4 R_H} \coth\left(\frac{\Delta t}{4 R_H} - i \epsilon\right) \right], \end{aligned} \quad (3.43)$$

with $\Lambda = L - 2|T - L/2|$. In the above, we approximated $\tau'' - \tau' \simeq \Delta t \sqrt{1 - R_H/\bar{R}}$ according to Eqs. (3.33) and the last equality follows from integration by parts in Δt (neglecting boundary terms).

The integral (3.43) can be computed by analytic continuation in the complex Δt plane in which, upon using the formula

$$\coth(\pi x) = \frac{1}{\pi x} - i \frac{x}{\pi} \sum_{n=-\infty}^{+\infty} \frac{1}{n(x - i n)}, \quad (3.44)$$

one finds the poles

$$\Delta t_n = 4 \pi n i R_H, \quad (3.45)$$

for any integer value of n . For $\Omega > 0$ (corresponding to emission) the contour of integration can be closed along an arc in the lower half plane and we get

$$P(2\Omega; t_1, L) \simeq N^2 \frac{\pi e^2 \hbar}{2m^2} \int_0^L \frac{dT |A_{0 \rightarrow 2}|^2}{R^6 \Omega^3 \sqrt{1 - R_H/R}} \sum_{n=1}^{N_L} e^{-8n\pi\Omega R_H \sqrt{1 - R_H/R}} + P_L, \quad (3.46)$$

where N_L is the maximum value of n for which the pole Δt_n lies within the contour of integration and P_L is the contribution from the arc.

If N_L is sufficiently large, then P_L can be neglected,

$$\sum_{n=1}^{N_L} e^{-8n\pi\Omega R_H \sqrt{1 - R_H/R}} \sim \frac{1}{e^{2\hbar\Omega/k_B\mathcal{T}} - 1}, \quad (3.47)$$

and one recovers the Planck distribution with (instantaneous) temperature

$$\mathcal{T} = \frac{T_H}{\sqrt{1 - R_H/R}}. \quad (3.48)$$

In general, however, one expects that the time L is not long enough and non-thermal contributions will render the evaluation of the probability of emission very complicated. One should then divide the time of collapse into small intervals and compute all the relevant quantities step by step. This procedure can be simplified by employing an approximation introduced in order to follow a trajectory [35] and which amounts to estimating the probability of emission per unit time at a given value of t (or τ) as

$$\frac{dP(\Omega; t)}{dL} \sim \frac{\pi e^2 \hbar}{2m^2} \frac{N^2 |A_{0 \rightarrow 2}|^2}{R^6 \Omega^3 \sqrt{1 - R_H/R}} \frac{1}{e^{2\hbar\Omega/k_B\mathcal{T}} - 1}, \quad (3.49)$$

in which all time-dependent quantities must be evaluated at the same time t and the right hand side is to lowest order in \dot{R} .

We finally recall that in Ref. [5] we proposed that the finite thickness of the macroshell could provide a solution to the problem of ultra-Planckian frequencies. In fact, if ω^* is the frequency of the emitted quanta as is measured by a distant observer, a fixed observer located near the point of emission at $r = R$ will instead measure a blue-shifted frequency

$$\omega = \left(1 - \frac{R_H}{R}\right)^{-1/2} \omega^*, \quad (3.50)$$

and this expression clearly gives $\omega > 1/\ell_p$ for R sufficiently close to R_H . In order to probe these modes, one should use a detector localized in a region smaller than $\omega^{-1} \sim \ell_p$, or, alternatively, one expects that the spread δ of the wavefunctions Φ_n should be less than ℓ_p for our collapsing microshells to couple with conformal quanta of ultra-Planckian energies. However, as we have shown in Refs. [39, 5], taking $\delta/\ell_p \rightarrow 0$ decouples the emitter from the radiation and ultra-Planckian frequencies are not excited (for a similar argument against ultra-Planckian frequencies, see Ref. [40]).

3.3 The flux

It is now straightforward to estimate the total flux of emitted radiation (the *luminosity*) as a function of time. In particular, the rate of proper energy lost by the macroshell per unit (Schwarzschild) time of a static observer placed at large r is given by

$$\frac{dE}{dt} = -\mathcal{A} \sum_{\omega} \mu(\omega) \Gamma(\omega) \hbar \omega \frac{dP(\omega; t)}{dL}, \quad (3.51)$$

where $\mathcal{A} = 4\pi R^2$ is the surface area of the shell, $\mu(\omega) = (1 - R_H/R)^{3/2} \omega^2$ the phase space measure for photons of frequency ω (measured at the shell position $r = R$), $\Gamma \sim 1$ the grey-body factor for zero angular momentum outgoing scalar waves [41] and the last factor is obtained from the approximation (3.49). The sum in Eq. (3.51) is dominated by the contribution with $\omega = 2\Omega$ and one obtains

$$\frac{dE}{dt} \simeq -\frac{16\pi^2 e^2}{9} \frac{N^2 \ell_m^2}{R^4} \left(\frac{\delta}{R_H} \right) \left(1 - \frac{R_H}{R} \right) \frac{\dot{R}^2}{e^2 \Omega \sqrt{1 - R_H/R/k_B T_H} - 1}. \quad (3.52)$$

We can now substitute the expressions (3.6) for Ω and (2.12) for δ and (minus) the flux becomes

$$\frac{dE}{dt} \simeq -\frac{16\pi^2 e^2}{9} \frac{N^2 \ell_m^{8/3}}{R^{10/3} R_H^{4/3}} \left(1 - \frac{R_H}{R} \right) \frac{\dot{R}^2}{e^2 \Omega \sqrt{1 - R_H/R/k_B T_H} - 1}. \quad (3.53)$$

We note that, for R close to R_H the Boltzmann exponent is very small (because of the Tolman factor). Upon expanding the exponent and keeping the leading order in $R - R_H$ we obtain

$$\frac{dE}{dt} \sim -e^2 \frac{N^2}{R^2} \left(\frac{\ell_m}{R_H} \right)^3 \left(1 - \frac{R_H}{R} \right)^{1/2} \dot{R}^2. \quad (3.54)$$

The flux should therefore vanish for $R \rightarrow R_H^+$ and, on comparing with the general relation given in Ref. [13],

$$\frac{dE}{dt} = \frac{\dot{R}_H}{2G} \frac{\sqrt{1 - R_H/R + \dot{R}^2} - \dot{R}}{\sqrt{1 - R_H/R + \dot{R}^2}} \simeq \frac{\dot{R}_H}{2G}, \quad (3.55)$$

one obtains, in the limit for R close to R_H ,

$$\dot{R}_H \sim -e^2 G \frac{N^2}{R^2} \left(\frac{\ell_m}{R_H} \right)^3 \left(1 - \frac{R_H}{R} \right)^{1/2} \dot{R}^2. \quad (3.56)$$

Were one to trust the above expression, one should then require that the energy-momentum tensor of the radiation remain locally finite when the shell approaches the surface $R = R_H^+$. This amounts to the condition [42],

$$\dot{R}_H \sim \left(1 - \frac{R_H}{R} \right)^\gamma, \quad \text{with } \gamma \geq 1. \quad (3.57)$$

radiation wavelength λ	$10^{-10} \div 10^{-7}$ cm
δ/λ	$10^{-3} \div 10^{-1}$
\dot{R}	$10^{-3} \div 10^{-2}$
total number of emissions	10^{39}
N_δ	$10^{35} \div 10^{36}$
total emitted energy	5% of $M_s(0)$

Table 1: Typical values of the relevant quantities resulting from the numerical analysis for $N = 2 \cdot 10^{40}$ microshells [$R_H(0) \simeq 4 \cdot 10^{-12}$ cm]. N_δ is the average number of emissions while the shell radius shrinks a space δ .

Since the quantity $B \sim 1$ near R_H , Eq. (3.55) would lead to the conclusion that the velocity of the macroshell satisfies

$$\dot{R}^2 \sim \left(1 - \frac{R_H}{R}\right)^\beta, \quad \text{with } \beta \geq \frac{1}{2}, \quad (3.58)$$

which means that the proper velocity \dot{R} should vanish at the horizon. Of course, the number of approximations we have employed does not allow one to consider the above a rigorous argument, but just a suggestive result. In particular, if the emission near the horizon is not thermal [N_L in Eq. (3.47) is small and just a few of the poles are included], the flux satisfies the condition (3.57) for any finite value of \dot{R} , the backreaction is reduced and our results are significantly modified only very close to the horizon where in any case our approximations break down. Indeed, we are only able to perform the analysis for R greater than a few times R_H and, in all the cases we consider, the microshells are confined with $\delta \ll R_H$.

3.4 The trajectory

One can now integrate numerically the equation of motion for the radius of the shell,

$$\dot{R}^2 = -1 + \frac{R_H^2}{(2GM)^2} + \frac{R_H}{2R} + \frac{G^2 M^2}{4R^2}, \quad (3.59)$$

together with Eq. (3.55) for R_H ,

$$\dot{R}_H \simeq -\frac{128\pi^3}{9} \alpha \frac{G N^2 \ell_m^{8/3}}{R^{10/3} R_H^{4/3}} \left(1 - \frac{R_H}{R}\right) \frac{\dot{R}^2}{e^{2\Omega} \sqrt{1 - R_H/R/k_B T_H} - 1}, \quad (3.60)$$

where $\alpha \equiv e^2/4\pi$.

Given our construction, the trajectories depend on the parameters N , α and the initial condition $R(0)$. In general, one finds that the non-adiabatic excitations occur relatively close to the horizon and there is no strong dependence on the initial value of R . In Fig. 6 we display the comparison between the trajectories computed from the above equations, with $N = 2 \cdot 10^{40}$ and various values of α , and that with constant $M_s = M$ (see also Table 1). Owing to our approximations, we are not able to display any reliable results as R gets close to R_H . The behaviour of R_H is shown in Fig. 7.

Increasing N requires an increase in α in order to preserve the difference between the radiating and the non-radiating trajectories (see Fig. 8 for a tenfold increase in N with respect to

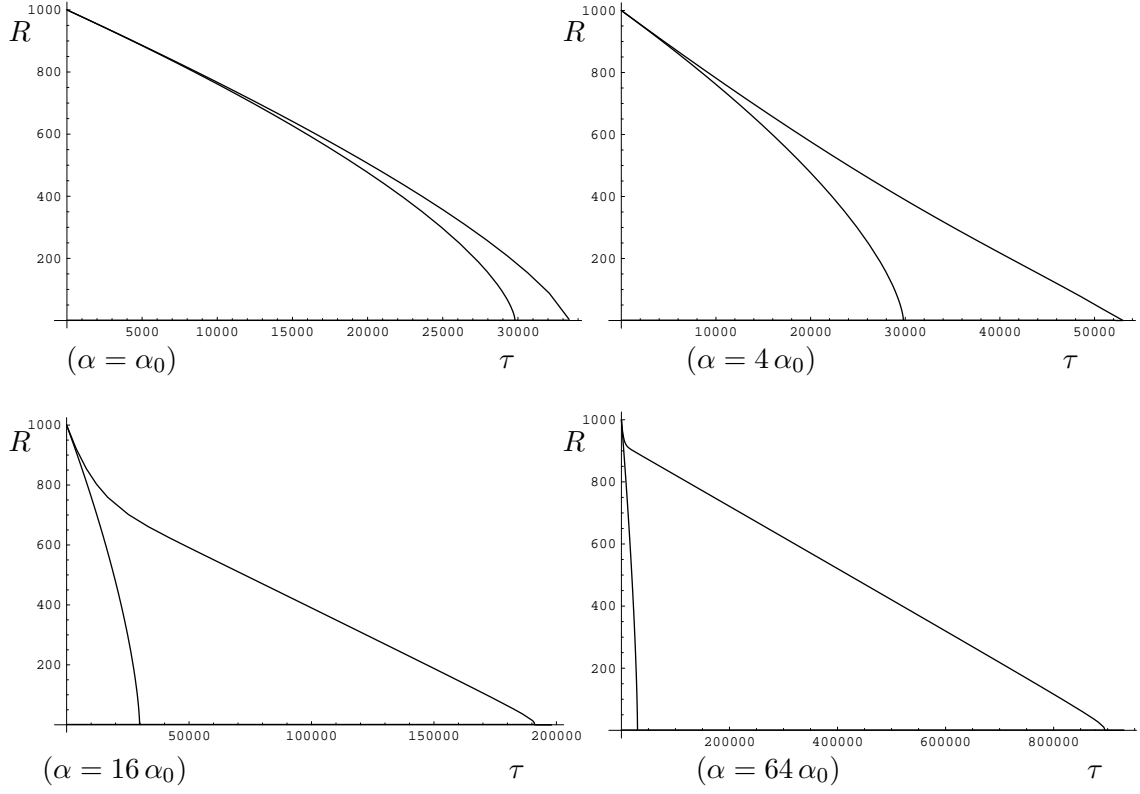


Figure 6: Trajectories of the radiating shell $R = R(\tau)$ in units of $R_H(0)$ with $N = 2 \cdot 10^{40}$ and four values of the coupling constant α (upper curves) compared to the non-radiating collapse (lower curves). All trajectories are evolved from $R(0) = 1000 R_H(0)$. The time τ , in all plots, is expressed in units of $2 \cdot 10^{-38} N \text{ GeV}^{-1}$ with $\hbar = c = 1$ and $\alpha_0 = 1.6 \cdot 10^{-33}$.

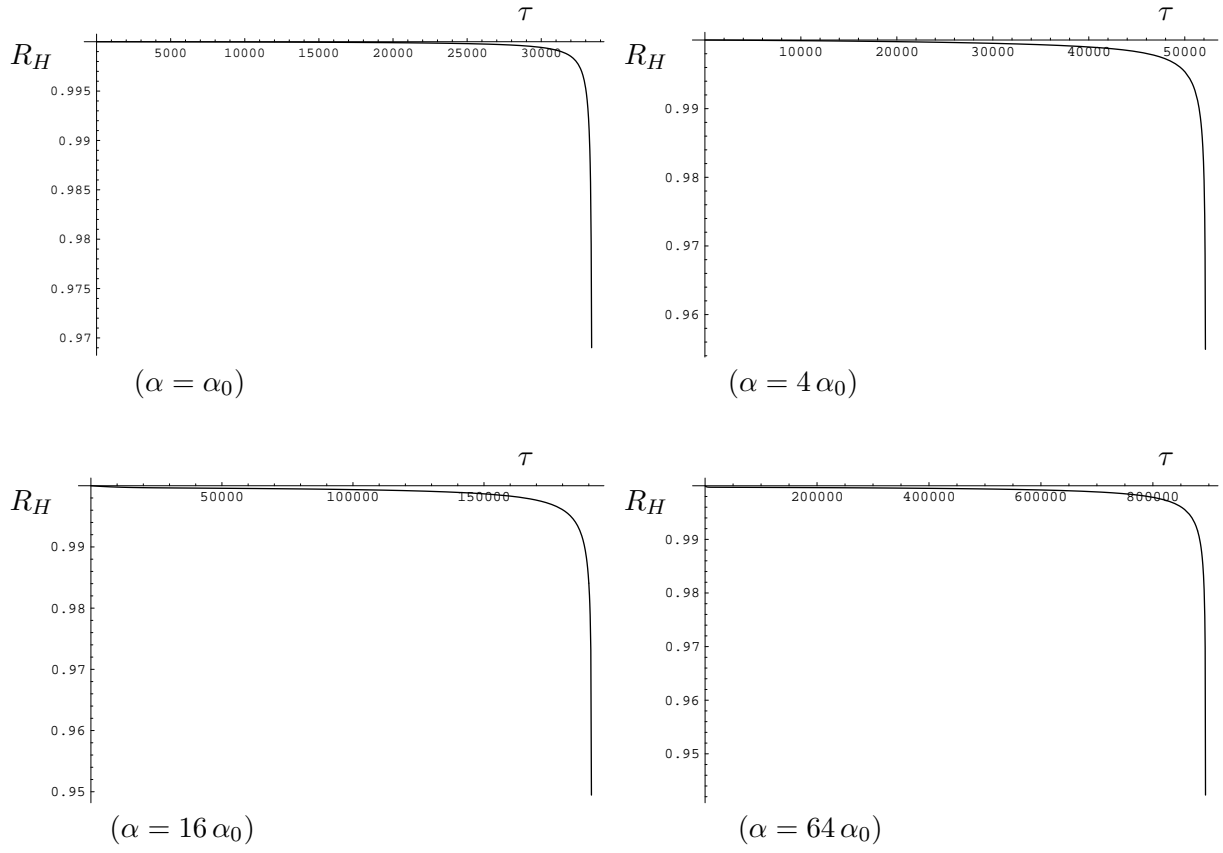


Figure 7: Behaviour of the gravitational radius for the radiating shell trajectories in Fig. 6.

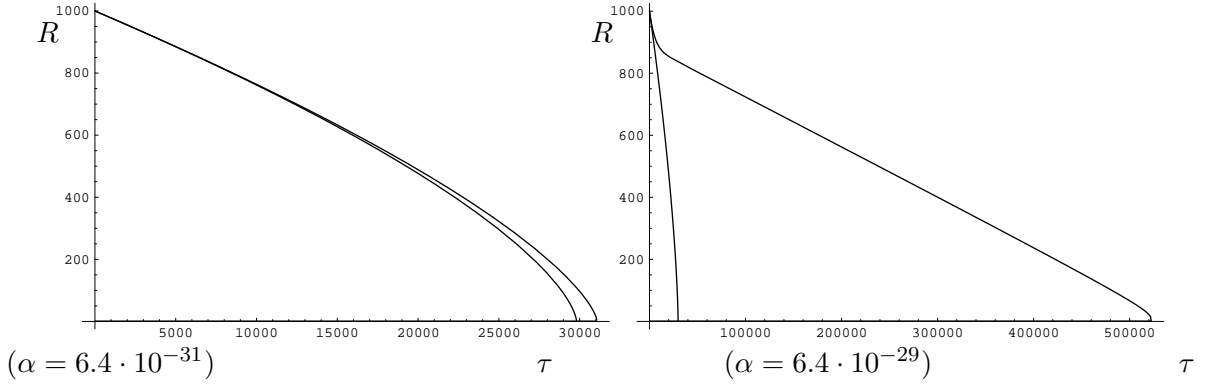


Figure 8: Trajectories of the radiating shell with $N = 2 \cdot 10^{41}$ and two values of the coupling constant α (upper curves) compared to the non-radiating collapse (lower curves).

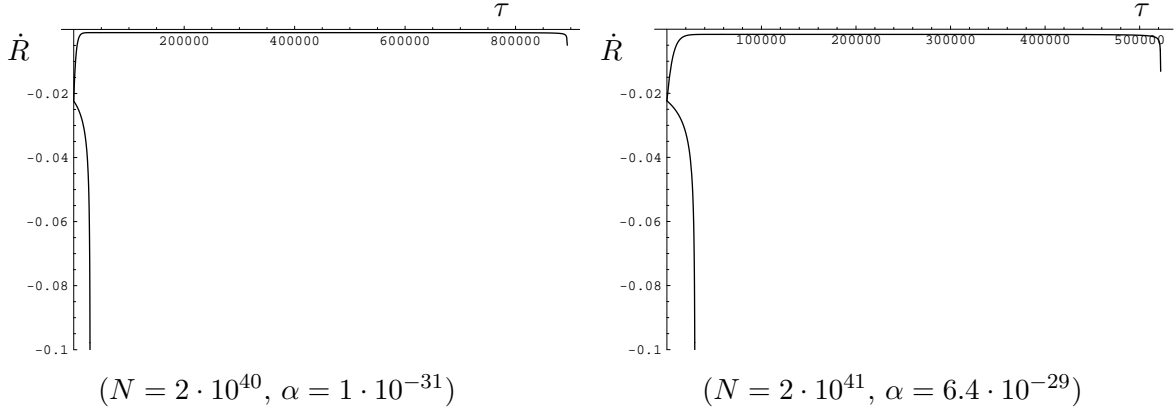


Figure 9: Velocity of the radiating shell for the fourth case of Fig. 6 and second case of Fig. 8 (upper curves) compared to the non-radiating collapse (lower curves).

Fig. 6). In fact, from Eq. (3.60), on setting $R \sim R_H \propto N m$ one finds (apart from dimensional constants)

$$\dot{R}_H \propto \frac{\alpha}{N^{8/3} m^{22/3}} , \quad (3.61)$$

which gives an estimate of how the effect scales with respect to the number of microshells, their mass m and the radiation coupling constant.

In Fig. 9 we plot the velocity \dot{R} of the collapsing shell (together with the velocity of the corresponding non-radiating shell) for two relevant cases. It is clear that \dot{R} remains (negative and) small (within a few percent of the speed of light), thus supporting our approximation scheme within which we just retain the lowest order in \dot{R} . In Fig. 10 the wavelength of emitted radiation quanta is plotted as a function of the time in order to show that it remains larger than δ (as given in Table 1).

Finally, we have also checked that on replacing the Bose-Einstein factor in Eq. (3.60) with the sum of just a few poles [see Eq. (3.47)] the evolution of the system is not substantially changed (only the backreaction is somewhat reduced).

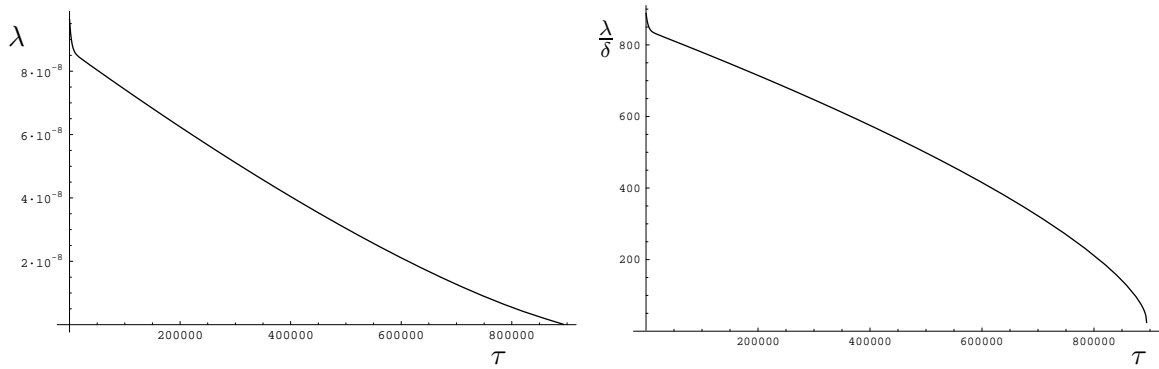


Figure 10: Wavelength λ of the emitted quanta and ratio λ/δ for the fourth case of Fig. 6.

4 Conclusions

In this paper we have analyzed the gravitational collapse (in the semiclassical approximation) of a macroshell built up of a (large) number of bosonic microshells (*s*-wave particles). Starting from the classical equations of motion, we obtained the potential and an effective Schrödinger equation for each microshell. The potential appearing in this equation ensures that the thickness of the macroshell does not increase significantly for a long enough piece of the trajectory, thus allowing one to take the thin shell limit at some point in the calculations. The time dependence of the potential leads to the non-adiabatic excitations (which we computed to leading order in the velocity of the macroshell) of the microshell bound states. On coupling the microshells to a scalar radiation field, we showed that the increase of kinetic energy can be radiated away and the emitted radiation is approximately thermal with a temperature given by the Tolman shifted instantaneous Hawking temperature (whether this mechanism can be related to the Hawking effect is a point which requires further study).

The effect is intrinsically quantum mechanical, since it is a consequence of the quantum mechanical-bound state nature of the macroshell and the coherence of the emitted radiation. This can cause the shell to lose enough energy so that the backreaction on the trajectory of the radius is large. For instance, for the case presented, the shell approaches the gravitational radius in a time which is more than an order of magnitude longer than the time a non-radiating shell would take to cross the horizon, and loses about five percent of its ADM mass as a burst of radiation (which is suggestive of the observed gamma-ray bursts [43]). One may also wonder at this point whether it is possible for the collapsing matter to produce enough radiation to reduce the energy of the shell so as to prevent the formation of an event horizon. Thus, if the ADM mass decreased fast enough, the shell itself would never reach the gravitational radius, unfortunately our approximations become unreliable as it is approached.

The model we have proposed clearly hinges on the formation of a condensate. Let us give some arguments in favour of this: of relevance for the latter is the fraction of microshells (particles) not in the condensate (ground state). This fraction is related to $(T/T_c)^\nu$, where T_c is the critical temperature for Bose-Einstein condensation and the (positive) exponent ν depends on the confining potential and the dimensionality of the system ⁶. For our case of about 10^{40}

⁶For example, $\nu = 3/2$ for a three-dimensional box and $\nu = 3$ for a three-dimensional harmonic trap (for a

particles and on setting $T = T_H$ (Hawking temperature) one has that $T_H/T_c < 10^{-10}$ which renders our description in terms of a condensate plausible.

Naturally, the relevance of our bosonic model for gravitational collapse which is expected to involve ordinary incoherent matter may be questioned. Moreover, it is clear that fermionic microshells would lead, because of the Pauli exclusion principle, to a much wider macroshell with and a loss of coherence. However, for a mixed fermion-boson system, one may just consider the bosonic part and apply our considerations to it since it will condensate in the lowest state. Certainly, the presence of fermionic and/or incoherent matter will reduce the effects we have illustrated. Nonetheless, one might even argue that an analogous phenomenon can happen for all collapsing bosonic matter, including the bosonic fraction of accretion disks around black holes. Our result would thus suggest a new mechanism by which the accreting matter can emit radiation.

Acknowledgement

We thank R. Brout for many enlighting discussions and clarifications.

A Microshell distribution and effective potential in NR

The NR for each microshell of rest mass m starting at large radius ($r_i \gg 2G M_s$) with negligible initial velocity can be obtained by setting $M_> - M_< = m$ and keeping terms up to first order in G and to leading order in m in the effective Hamiltonian constraint (2.4). The total energy of the system is thus given by the sum of the kinetic energies of all microshells and mutual interaction potential energies. The latter can be written, on introducing relative (\bar{r}_i) and centre-mass (R) coordinates, as [9]

$$V(r_1, \dots, r_N) = -G \frac{M^2}{2R} + G \frac{m^2}{2R^2} \sum_{i < j}^N |\bar{r}_i - \bar{r}_j|. \quad (\text{A.1})$$

Unfortunately, this potential does not allow for an analytic treatment of the complete problem, therefore we shall apply an analogous procedure to that followed in Section 2 in order to obtain a Schrödinger equation for each microshell in the mean field of the others.

Let us first try with a configuration $\{r_i, M_i\}_{hom}$ in which $N - 1$ microshells have equally spaced radii, $r_i = r_1 + (i - 1)\delta/(N - 1)$, so that $M_i = m[(r_i - r_1)(N - 1)/\delta + 1]$. Hence, the equation of motion (2.3) in NR for the N^{th} microshell with radius $r_1 < x < r_{N-1}$ becomes

$$\frac{1}{2}m \left(\frac{dx}{dt} \right)^2 \simeq G \frac{m^2}{x} \left(N \frac{x - r_1}{\delta} + 1 \right), \quad (\text{A.2})$$

where $t \equiv \tau_x$ is the Newtonian time. Changing to the relative coordinate $\bar{x} = x - R$, one obtains

$$H_m \simeq \frac{1}{2}m \left(\frac{d\bar{x}}{dt} \right)^2 + G \frac{mM}{R} \frac{\bar{x}}{\delta} \left(\frac{\bar{x}}{R} - 1 \right), \quad (\text{A.3})$$

where we have used $|\bar{x}| \ll R$ and omitted all potential terms which do not contain \bar{x} (they would just contribute to the ground state energy in the Schrödinger equation). It is clear that

review, see Ref. [44]).

the potential above for $\bar{x} = \pm\delta/2$ does not match smoothly with the NR limit of the external potential given in Eq. (2.9) because of the term linear in \bar{x} . This means that the configuration $\{r_i, M_i\}_{hom}$ is not stable. In fact, the minimum of the potential is not at the origin $\bar{x} = 0$, and one then expects the microshells to move away from the above configuration.

In order to obtain an internal configuration compatible with the external potential, let us assume a potential with a minimum at $\bar{x} = 0$ (as is required by the symmetry of the external potential) and consider small oscillations about this equilibrium point. Such oscillations will be harmonic and the potential to lowest order is given by

$$V_{NR} = G \frac{M m}{2 R^2 \delta} (x - R)^2 + C_1 , \quad (\text{A.4})$$

where C_1 is a constant. If we assume $M_{i+1} = M_i + m$, for the most likely configuration $\{r_i, M_i\}$, r_i can be determined by comparing the potential V_{NR} with the one obtained from the NR limit of Eq. (2.3), to wit

$$V'_{NR} = G \frac{m(m - 2M_i)}{2x} + C_2 , \quad r_i < x < r_{i+1} , \quad (\text{A.5})$$

where C_2 is another constant. On equating the potentials V_{NR} and V'_{NR} in the limit $x \rightarrow r_i^+$ (from above) and setting $C = C_2 - C_1$, one obtains

$$2M_i - m = r_i^+ \left[\frac{2C}{Gm} - \frac{M}{R^2 \delta} (r_i^+ - R)^2 \right] . \quad (\text{A.6})$$

Then, on defining $r_{i+1} = r_i + y_i$ and subtracting the same expression for $x \rightarrow r_{i+1}^+$, one has

$$\begin{aligned} 2m &= 2M_{i+1} - 2M_i \\ &= \frac{2C}{Gm} y_i + \frac{M r_i^+}{R^2 \delta} \left[(r_i^+ - R)^2 - (r_i^+ + y_i - R)^2 \right] - \frac{y_i M}{R^2 \delta} (r_i^+ + y_i - R)^2 \\ &= \frac{2C}{Gm} y_i - \frac{y_i M}{R^2 \delta} \left[R^2 - 4r_i^+ R + 3(r_i^+)^2 + y_i (3r_i^+ - 2R + y_i) \right] . \end{aligned} \quad (\text{A.7})$$

The first term on the right hand side corresponds to the homogeneous distribution if the constant $C = Gm^2(N - 1)/\delta$. In general, however, the other terms cannot be neglected, so that the microshells are not equally spaced. Further, the y_i can be computed recursively for $i = 1, 2, \dots, N - 2$ on making use of Eq. (A.7) and the condition $r_1 \equiv R - \delta/2$ (which determines the constant C). In any case, as we discuss in Appendix C, the actual quadratic or linear structure of the potential inside the macroshell has little influence on the energy levels of the lowest states.

B Shell dynamics in Schwarzschild time

It is known that, even if two theories are classically equivalent, their quantization may lead to different Hilbert spaces and, therefore, different quantum pictures and that this problem is potentially present in Einstein's gravity (see, *e.g.*, Ref. [30]). It is thus interesting to compare the potential $V_m^{(\tau)}$ obtained in Section 2 with the one corresponding to a foliation of space-time into slices parameterized by the Schwarzschild time $t_\infty \equiv t_N$ measured by a (distant) static observer.

Given this potential, one can (in principle) construct the Hilbert space \mathcal{H}_τ and compute any observable in order to check the equivalence of \mathcal{H}_τ and \mathcal{H}_t . Unfortunately, the form of the potential we obtain in the following makes the explicit construction practically impossible.

First we observe that the proper time of the test shell can be expressed in terms of the inner and outer Schwarzschild times $t_<$ and $t_> \equiv t_x$ (see Fig. 1) by making use of

$$\begin{aligned} d\tau_x^2 &= \left(1 - \frac{2GM_<}{x}\right) dt_<^2 - \left(1 - \frac{2GM_<}{x}\right)^{-1} dx^2 \\ &= \left(1 - \frac{2GM_>}{x}\right) dt_>^2 - \left(1 - \frac{2GM_>}{x}\right)^{-1} dx^2, \end{aligned} \quad (\text{B.1})$$

which yields the ratio

$$\left(\frac{dt_<}{dt_>}\right)^2 = \frac{x - 2GM_>}{x - 2GM_<} - \frac{2x^2 G(M_> - M_<)}{(x - 2GM_>)(x - 2GM_<)^2} \left(\frac{dx}{dt_>}\right)^2, \quad (\text{B.2})$$

where, from Eq. (2.3),

$$\left(\frac{dx}{dt_>}\right)^2 = \frac{1}{x} \frac{(x - 2GM_>)^2 F(x)}{x - 2GM_> + xF(x)}. \quad (\text{B.3})$$

These expressions can be iterated for each microshell with radius $x < r_i \leq r_N$ and, together with (B.1), yield

$$\begin{aligned} \left(\frac{d\tau_x}{dt_\infty}\right)^2 &= \left[\left(1 - \frac{2GM_x}{x}\right) + \left(1 - \frac{2GM_x}{x}\right)^{-1} \left(\frac{dx}{dt_x}\right)^2 \right] \\ &\times \prod_{i=x+1}^N \left[\frac{r_i - 2GM_{i-1}}{r_i - 2GM_{i-1}} - \frac{2r_i^2 G(M_i - M_{i-1})}{(r_i - 2GM_i)(r_i - 2GM_{i-1})^2} \left(\frac{dr_i}{dt_i}\right)^2 \right] \\ &= \left[\left(1 - \frac{2GM_x}{x}\right) + \frac{(x - 2GM_x)F(x)}{x - 2GM_x + xF(x)} \right] \\ &\times \prod_{i=x+1}^N \left[\frac{r_i - 2GM_{i-1}}{r_i - 2GM_{i-1}} + \frac{2r_i^2 G(M_i - M_{i-1})(r_i - 2GM_i)F(r_i)}{(r_i - 2GM_{i-1})^2 [r_i - 2GM_i + r_i F(r_i)]} \right], \end{aligned} \quad (\text{B.4})$$

where r_{x+1} is the radius of the first microshell having radius greater than that of the test shell and

$$F(r_i) = -1 + \frac{(M_i - M_{i-1})^2}{m^2} + G \frac{M_i + M_{i-1}}{r_i} + G^2 \frac{m^2}{4r_i^2}. \quad (\text{B.5})$$

On then multiplying Eq. (2.3) by $m/2$ and using Eq. (B.4), one obtains the equation of motion for the microshell in the form of an effective Hamiltonian constraint in the Schwarzschild time

$$H_m^{(t)} \equiv \frac{1}{2} m \left(\frac{dx}{d\tau_x}\right)^2 \left(\frac{d\tau_x}{dt_\infty}\right)^2 + V^{(t)} = 0. \quad (\text{B.6})$$

The explicit form of $V^{(t)}$ now depends both on the distribution $\{r_i, M_i\}$ of the microshells inside the macroshell and the cumbersome time conversion factor in Eq. (B.4).

Hence, we again rely on the thin shell limit ($\delta \ll r_1$) and consider the form of the potential when $x < r_1$ or $x > r_N$. For $x < X$ one finds [see case (1) in Fig. 2]

$$\left\{ \begin{array}{l} \left(\frac{dx}{dt_\infty} \right)^2 = \left[1 - \frac{2Gm}{x} + \frac{(x - 2Gm)F_<(x)}{x - 2Gm + xF_<(x)} \right] \\ \quad \times \left[\frac{X - 2GM_s}{X - 2Gm} + \frac{2XG(M_s - m)(X - 2GM_s)F_<(X)}{(X - 2Gm)^2[X - 2GM_s + XF_<(X)]} \right] F_<(x) \\ \left(\frac{dX}{dt_\infty} \right)^2 = \left[1 - \frac{2GM_s}{X} + \frac{(X - 2GM_s)F_<(X)}{X - 2GM_s + XF_<(X)} \right] F_<(X) . \end{array} \right. \quad (\text{B.7})$$

Analogously, for $x > X$ [see case (2) in Fig. 2]

$$\left\{ \begin{array}{l} \left(\frac{dX}{dt_\infty} \right)^2 = \left[1 - \frac{2G(M_s - m)}{X} + \frac{[X - 2G(M_s - m)]F_>(X)}{X - 2G(M_s - m) + XF_>(X)} \right] \\ \quad \times \left[\frac{x - 2GM_s}{x - 2G(M_s - m)} + \frac{2xGm(x - 2GM_s)F_>(x)}{[x - 2G(M_s - m)]^2[x - 2GM_s + xF_>(x)]} \right] \\ \quad \times F_>(X) \\ \left(\frac{dx}{dt_\infty} \right)^2 = \left[1 - \frac{2GM_s}{x} + \frac{(x - 2GM_s)F_>(x)}{x - 2GM_s + xF_>(x)} \right] F_>(x) , \end{array} \right. \quad (\text{B.8})$$

where $F_<$ and $F_>$ have been given in Eqs. (2.5) and (2.6). On introducing the relative (\bar{r}) and centre-mass (R) radii, after some lengthy algebra one obtains an effective Hamiltonian for the two shells given by

$$H^{(t)} = \frac{1}{2}M \left(\frac{dR}{dt_\infty} \right)^2 + \frac{1}{2}\mu \left(\frac{d\bar{r}}{dt_\infty} \right)^2 + V^{(t)} \equiv H_M^{(t)} + H_m^{(t)} , \quad (\text{B.9})$$

where the potential can be expanded in powers of G and \bar{r}/R according to

$$V^{(t)} = \sum_{n=0}^{\infty} G^n \sum_{k=0}^{\infty} V_{n,k}(M, m; M_s; R) \left(\frac{\bar{r}}{R} \right)^k . \quad (\text{B.10})$$

Only the terms linear in \bar{r}/R are relevant for our calculation and, to leading order in G , they are given by

$$V_{1,1} = \frac{M_s m}{2R} \times \left\{ \begin{array}{ll} \left(4 \frac{M_s^2}{M^2} - 4 \frac{M_s}{M} - 8 + 6 \frac{M}{M_s} + 6 \frac{M^2}{M_s^2} - 2 \frac{M^3}{M_s^3} - \frac{M^4}{M_s^4} \right) & \bar{r} > +\frac{\delta}{2} \\ \left(4 \frac{M_s^2}{M^2} - 10 + 6 \frac{M^2}{M_s^2} - \frac{M^4}{M_s^4} \right) & \bar{r} < -\frac{\delta}{2} , \end{array} \right. \quad (\text{B.11})$$

where we have again neglected non-leading terms in m .

On interpolating between the two terms given by $V_{1,1}$ in Eq. (B.11), we obtain

$$H_m^{(t)} = \frac{1}{2}m \left(\frac{d\bar{r}}{dt_\infty} \right)^2 + V_m^{(t)} , \quad (\text{B.12})$$

with the potential

$$V_m^{(t)} = G \frac{M_s m \bar{r}^2}{2 R^2 d} \left(-2 \frac{M_s}{M} + 1 + 3 \frac{M}{M_s} - \frac{M^3}{M_s^3} \right) + G \frac{M_s m \bar{r}}{2 R^2} \left(4 \frac{M_s^2}{M^2} - 2 \frac{M_s}{M} - 18 + 3 \frac{M}{M_s} + 6 \frac{M^2}{M_s^2} - \frac{M^3}{M_s^3} - \frac{M^4}{M_s^4} \right), \quad (\text{B.13})$$

which holds for $|r| < \delta/2$.

If we now take the thin shell limit of $V_m^{(t)}$ only the linear part $V_{1,1}$ survives. We can then compare the result with the corresponding linear part of $V_m^{(\tau)}$, as computed in Section 2, using the Schwarzschild time, and then obtaining

$$V_m^{(\tau)}(t) = V_m^{(\tau)} \left(\frac{d\tau}{dt_\infty} \right)^2, \quad (\text{B.14})$$

where

$$\left(\frac{d\tau}{dt_\infty} \right)^2 = \left[1 - \frac{2 G M_s}{R} + \frac{(R - 2 G M_s) F(R)}{R - 2 G M_s + R F(R)} \right], \quad (\text{B.15})$$

and

$$F(R) = -1 + \frac{M_s^2}{M^2} + G \frac{M_s}{R} + \frac{G^2 M^2}{4 R^2}. \quad (\text{B.16})$$

This yields, to lowest order in G ,

$$V_m^{(\tau)}(t) \simeq G \frac{M_s m |\bar{r}|}{2 R^2} \left(2 - \frac{M^2}{M_s^2} \right), \quad (\text{B.17})$$

which coincides with the thin shell limit (*i.e.*, linear part) of $V_m^{(t)}$, Eq. (B.13), for $M = M_s$. This shows that the effective potential governing the motion of the microshells is the same in NR for the two foliations $\{\Sigma_t\}$ and $\{\Sigma_\tau\}$.

C Microshell confinement

We shall now show that the expression for the macroshell thickness δ in Eq. (2.12) can be obtained within the adiabatic approximation (R constant) in NR by either considering just the linear part of the potential $V_m^{(\tau)}$ in $H_m^{(\tau)}$ (thus neglecting the details of the distribution of the microshells) or just the quadratic part (which is related to a given distribution of microshells, see Appendix A). From the Hamiltonian $H_m^{(\tau)}$ one can obtain a (time-independent) Schrödinger equation

$$\left[\frac{\hat{\pi}_r^2}{2m} + V_{(i)} \right] \Phi_n = E_n \Phi_n, \quad (\text{C.1})$$

where $\hat{\pi}_r = -i \hbar \partial_r$ and, on retaining the linear part, one has ($N m \equiv M = M_s$)

$$V_{(1)} = \frac{G N m^2}{2 R} \frac{|\bar{r}|}{R}, \quad (\text{C.2})$$

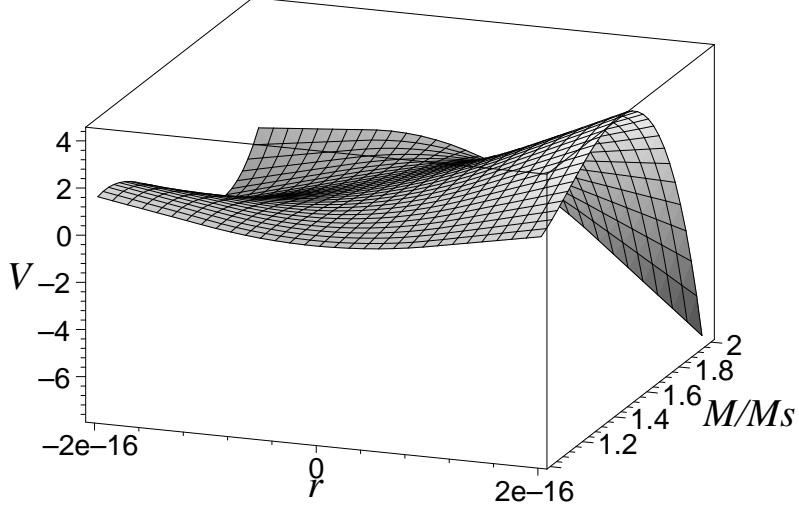


Figure 11: The potential $V_m^{(t)}$ at order G^2 for $M = 10^{40} m_h$ and $\delta = \ell_h = 10^{-16} \text{ m}$ $1 \leq M/M_s \leq 2$. Vertical units are arbitrary.

or, on considering the quadratic term,

$$V_{(2)} = \frac{G N m^2}{2 R^2} \frac{\bar{r}^2}{\delta} . \quad (\text{C.3})$$

Solutions to Eq. (C.1) with $V_{(i)} = V_{(1)}$ are given (apart from a normalization factor) by the Airy function Ai [45],

$$\Phi_n^{(1)} = \begin{cases} \text{Ai}(\xi - \xi_{2k}) & n = 2k \\ \text{sgn}(\bar{r}) \text{Ai}(\xi - \xi_{2k+1}) & n = 2k + 1 , \end{cases} \quad (\text{C.4})$$

where $k \in \mathbb{N}$ and $\xi \equiv (2 G N m^3 / \hbar^2 R^2)^{1/3} \bar{r}$. The ξ_{2k+1} are the zeros of the Airy function, $\text{Ai}(-\xi_{2k+1}) = 0$, and ξ_{2k} the zeros of its first derivative, $\text{Ai}'(-\xi_{2k}) = 0$. The corresponding eigenvalues are given by

$$E_n^{(1)} = m \left(\frac{N \ell_p^2}{R^2} \right)^{2/3} \frac{\xi_n}{2^{1/3}} , \quad (\text{C.5})$$

and the spread of such states (for n small) is well approximated by Eq. (2.12).

Solutions for $V_{(i)} = V_{(2)}$ are given instead by the usual harmonic oscillator wavefunctions (again we omit normalization factors),

$$\Phi_n^{(2)} = H_n(\zeta) e^{-\zeta^2} , \quad (\text{C.6})$$

where $\zeta \equiv (G N m^3 / 2 \hbar^2 R^2 \delta)^{1/4} \bar{r}$ and H_n are Hermite polynomials [45]. The energy eigenvalues are

$$E_n^{(2)} = \sqrt{\frac{\hbar N m}{2 \delta}} \frac{\ell_p}{R} \left(n + \frac{1}{2} \right) . \quad (\text{C.7})$$

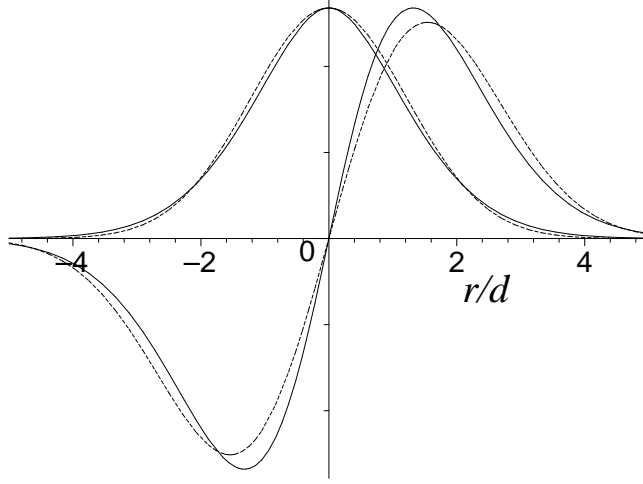


Figure 12: Plot of $\Phi_n^{(1)}$ (continuous lines) and $\Phi_n^{(2)}$ (dotted lines) for $n = 0, 1$. Vertical units are arbitrary and d should be δ .

If we now substitute the expression for δ previously obtained, we get the energy spectrum

$$E_n^{(2)} = m \left(\frac{N \ell_p^2}{R^2} \right)^{2/3} \left(\frac{n}{2^{1/3}} + \frac{1}{2^{4/3}} \right), \quad (\text{C.8})$$

which is of the same order of magnitude as Eq. (C.5). Also, the spread of such $\Phi_n^{(2)}$ for n small is again given by Eq. (2.12) (see also Fig. 12) and we can therefore represent the state of each microshell either by using $\Phi_n^{(1)}$ or $\Phi_n^{(2)}$.

It is also important to observe that the energy gap between two adjacent states,

$$\Delta E \sim \left(\frac{N \ell_p^2}{R^2} \right)^{2/3} m \sim \left(\frac{\ell_m R_H}{R^2} \right)^{2/3} m, \quad (\text{C.9})$$

is much smaller than m for $R \geq R_H$, which suggests that outside the gravitational radius the effects considered in the present paper dominate over the microshell creation studied in Ref. [9].

We may also see the small difference between the energy levels in the two cases by employing a W.K.B. quantization [9]. Indeed if we require

$$\oint \pi_r d\bar{r} = m \oint \dot{\bar{r}} d\bar{r} = \left(n + \frac{1}{2} \right) h, \quad (\text{C.10})$$

for both potentials and consider cycles within the potential well, that is the amplitude of the oscillations will correspond to the width of the shell, one has

$$m \oint \dot{\bar{r}} d\bar{r} = \sqrt{2m} \int_{-\delta/2}^{+\delta/2} d\bar{r} \left[V_{(i)}(\delta/2) - V_{(i)}(\bar{r}) \right]^{1/2} = \left(n + \frac{1}{2} \right) h, \quad (\text{C.11})$$

thus determining $\delta_{(1)}$ and $\delta_{(2)}$ for the linear and quadratic potentials respectively. One obtains

$$\begin{aligned}\delta_{(1)} &= 2 \left[\frac{3}{2} \left(n + \frac{1}{2} \right) h \left(\frac{R^2}{16 G M m} \right)^{1/2} \right]^{2/3} \\ \delta_{(2)} &= 2 \left[\frac{4\sqrt{2}}{\pi} \left(n + \frac{1}{2} \right) h \left(\frac{R^2}{16 G M m} \right)^{1/2} \right]^{2/3},\end{aligned}\tag{C.12}$$

and correspondingly a binding energy

$$\begin{aligned}E_n^{(1)} &= \left(\frac{9}{128} \right)^{1/3} \left[\left(n + \frac{1}{2} \right) h \right]^{2/3} \left(\frac{G M}{2 R^2} \right)^{2/3} m \\ E_n^{(2)} &= \left(\frac{1}{\pi^2} \right)^{1/3} \left[\left(n + \frac{1}{2} \right) h \right]^{2/3} \left(\frac{G M}{2 R^2} \right)^{2/3} m,\end{aligned}\tag{C.13}$$

which are of the same order of magnitude and we have added to $E_n^{(2)}$ the additional $\mathcal{O}(G)$ term in Eq. (2.11) so as to have continuity of the potentials at $|\bar{r}| = \delta/2$. It is clear that in both cases we have allowed for a maximal oscillation of the test microshell and thus obtained $\delta_{(i)}$.

Finally, let us now check how close to the gravitational radius we can use the bound states obtained above. From Eq. (2.9) one finds that $V^{(\tau)}$ is always positive for $\bar{r} < 0$, but becomes negative for $\bar{r} > 0$ if

$$R < \frac{G^2 M^2}{2 R_H} \equiv R_C,\tag{C.14}$$

As a sufficient condition for applicability of the modes $\Phi_n^{(i)}$, we shall require that the energy be less than the value of the potential for $\bar{r} \sim 4\delta$ (see Fig. 12), *i.e.*, $E_n^{(i)} < V_{(1)}(\bar{r} = 4\delta)$. The above condition implies $n < 4$ for $R > R_H$ ($> R_C$) and is therefore satisfied for the second excited state ($n = 2$) we use in Section 3, otherwise the shell breaks up.

References

- [1] P.S. Joshi, *Pramana* **55**, 529 (2000) [gr-qc/0006101].
- [2] S.W. Hawking, *Nature* **248**, 30 (1974) and *Comm. Math. Phys.* **43**, 199 (1975).
- [3] P. Hajicek, *Phys. Rev. D* **36**, 1065 (1987).
- [4] S.W. Hawking and G.F.R. Ellis, *The large scale structure of space-time* (Cambridge, Cambridge University Press, 1973)
- [5] R. Casadio and G. Venturi, *Class. Quantum Grav.* **13**, 2715 (1996).
- [6] R. Casadio, *Nucl. Phys. B (Proc Suppl)* **57**, 177 (1997).
- [7] R. Casadio, F. Finelli, and G. Venturi, *Class. Quantum Grav.* **15**, 2451 (1998).

- [8] F. Finelli, G.P. Vacca, and G. Venturi, Phys. Rev. D **58**, 103514 (1998).
- [9] G.L. Alberghi, R. Casadio, G.P. Vacca, and G. Venturi, Class. Quantum Grav. **16**, 131 (1999).
- [10] R. Brout and G. Venturi, Phys. Rev. D **15**, 2436 (1989).
- [11] C. Bertoni, F. Finelli, and G. Venturi, Class. Quantum Grav. **13**, 2375 (1996).
- [12] R. Casadio, Int. Jour. Mod. Phys. D **9**, 511 (1998).
- [13] G.L. Alberghi, R. Casadio, and G. Venturi, Phys. Rev. D **60**, 124018 (1999).
- [14] R. Casadio, Nucl. Phys. **B** (Proc Suppl) **88**, 273 (2000).
- [15] N.D. Birrell and P.C.W. Davis, *Quantum fields in curved space* (Cambridge, Cambridge University Press, 1982)
- [16] S.W. Hawking, Phys. Rev. D **14**, 2460 (1976).
- [17] J.D. Bekenstein, Phys. Rev. D **7**, 2333 (1973).
- [18] K.S. Thorne, R.H. Price, and D.A. MacDonald, eds. *Black holes: the membrane paradigm* (New Heaven, Yale University Press, 1986)
- [19] S. Carlip, Phys. Rev. Lett. **82**, 2828 (1999).
- [20] A. Ashtekar, Class. Quantum Grav. **17**, 253 (2000).
- [21] G. 't Hooft, Nucl. Phys. **B 355**, 138 (1990).
- [22] P. Hajicek, Nucl. Phys. **B** (Proc Suppl) **88**, 114 (2000).
- [23] P. Hajicek, Nucl. Phys. **B 603**, 555 (2001); P. Hajicek and K. Kiefer, Nucl. Phys. **B 603**, 531 (2001).
- [24] D.G. Boulware, Phys. Rev. D **13**, 2169 (1976); U.H. Gerlach, Phys. Rev. D **14**, 1479 (1976).
- [25] S. Sonogo, J. Almergren, and M.A. Abramowicz, Phys. Rev. D **62**, 064010 (2000).
- [26] Y. Oshiro, S. Konno, K. Nakamura, and A. Tomimatsu, Prog. Theor. Phys. **89**, 77 (1993).
- [27] E.W. Mielke and F.E. Schunk, *Boson stars: early history and recent prospects*, gr-qc/9801063.
- [28] W. Israel, Nuovo Cimento **B 44**, 1 (1966) and Nuovo Cimento **B 48**, 463 (1966).
- [29] C.W. Misner, K.S. Thorne, and J.A. Wheeler, *Gravitation* (San Francisco: Freeman, 1973)
- [30] P. Hajicek and J. Kiowski, Phys. Rev. D **61**, 024037 (2000).
- [31] C. M. Will, *Theory and experiment in gravitational physics* (Cambridge, Cambridge University Press, 1993)

- [32] A. Messiah, *Quantum mechanics* (North-Holland Publishing Co., Amsterdam, 1961); S. Schweber, *An introduction to quantum field theory* (Harper and Row, New York, 1961).
- [33] H.R. Lewis and W.B. Riesenfeld, J. Math. Phys. **10**, 1458 (1969).
- [34] X.C. Gao, J.B. Xu, and T.Z. Quian, Phys. Rev. A **44**, 7016 (1991).
- [35] R. Casadio and G. Venturi, Phys. Lett. **A 252**, 109 (1999).
- [36] P.C. Vaidya, Proc. Indian Acad. Sci. **A33**, 264 (1951).
- [37] W. Israel, Phys. Lett. **24A**, 184 (1967) and Phys. Rev. **143**, 1016 (1966).
- [38] R. Brout and R. Parentani, Nucl. Phys. **B 383**, 474 (1992).
- [39] R. Casadio and G. Venturi, Phys. Lett. **A 199**, 33 (1995).
- [40] A.D. Helfer, *Trans-Planckian modes, back-reaction, and the Hawking process*, gr-qc/0008016 (2000).
- [41] D.N. Page, Phys. Rev. D **13**, 198 (1976).
- [42] S.M. Christensen and S.A. Fulling, Phys. Rev. D **15**, 2088 (1977).
- [43] A.J. Castro-Tirado, *Observations and theoretical models of Gamma-Ray Bursts*, to appear in the Proceedings of the 4th INTEGRAL Workshop, astro-ph/0102122; T. Piran, *Gamma-Ray Bursts - when the theory meets observation*, astro-ph/0104134.
- [44] F. Dalfovo, S. Giorgini, L.P. Pitaevskii, and S. Stringari, *Rev. Mod. Phys.*, **71** (1999) 463.
- [45] M.A. Abramowitz and I.A. Stegun, *Handbook of mathematical functions* (New York, Dover, 1972)